Nonspherical Nanoparticle Shape Stability Is Affected by Complex Manufacturing Aspects: Its Implications for Drug Delivery and Targeting

Bernard Manuel Haryadi,* Daniel Hafner, Ihsan Amin, Rene Schubel, Rainer Jordan, Gerhard Winter, and Julia Engert

The shape of nanoparticles is known recently as an important design parameter influencing considerably the fate of nanoparticles with and in biological systems. Several manufacturing techniques to generate nonspherical nanoparticles as well as studies on in vitro and in vivo effects thereof have been described. However, nonspherical nanoparticle shape stability in physiological-related conditions and the impact of formulation parameters on nonspherical nanoparticle resistance still need to be investigated. To address these issues, different nanoparticle fabrication methods using biodegradable polymers are explored to produce nonspherical nanoparticles via the prevailing film-stretching method. In addition, systematic comparisons to other nanoparticle systems prepared by different manufacturing techniques and less biodegradable materials (but still commonly utilized for drug delivery and targeting) are conducted. The study evinces that the strong interplay from multiple nanoparticle properties (i.e., internal structure, Young's modulus, surface roughness, liquefaction temperature [glass transition (T_g) or melting (T_m)], porosity, and surface hydrophobicity) is present. It is not possible to predict the nonsphericity longevity by merely one or two factor(s). The most influential features in preserving the nonsphericity of nanoparticles are existence of internal structure and low surface hydrophobicity (i.e., surface-free energy (SFE) > ≈55 mN m^{-1}, material–water interfacial tension <6 mN m^{-1}), especially if the nanoparticles are soft (<1 GPa), rough (R_{rms} > 10 nm), porous (>1 m^2 g^{-1}), and in possession of low bulk liquefaction temperature (<100 °C). Interestingly, low surface hydrophobicity of nanoparticles can be obtained indirectly by the significant presence of residual stabilizers. Therefore, it is strongly suggested that nonsphericity of particle systems is highly dependent on surface chemistry but cannot be appraised separately from other factors. These results and reviews allot valuable guidelines for the design and manufacturing of nonspherical nanoparticles having adequate shape stability, thereby appropriate with their usage purposes. Furthermore, they can assist in understanding and explaining the possible mechanisms of nonspherical nanoparticles effectivity loss and distinctive material behavior at the nanoscale.

B. M. Haryadi, Prof. G. Winter, Prof. J. Engert[+]
Pharmaceutical Technology and Biopharmaceutics
Department of Pharmacy
Ludwig-Maximilians-Universität München
Butenandtstraße 5, 81377 Munich, Germany
E-mail: bernard-manuel.haryadi@cup.uni-muenchen.de,
bmharyadi@gmail.com
D. Hafner, Dr. I. Amin,[++] R. Schubel, Prof. R. Jordan
Department of Chemistry
Dresden University of Technology
Mommsenstraße 4, 01069 Dresden, Germany

[+]Present address: Regional Office for Health and Social Affairs Berlin (LAGeSo), Turmstraße 21, 10559 Berlin, Germany
[++]Present address: Leibniz-Institute for Plasma Science and Technology (INP) Greifswald, Felix-Hausdorff-Straße 2, 17489 Greifswald, Germany

1. Introduction

For a long time, biodegradable nanoparticle drug delivery systems have been investigated for numerous applications such as cancer treatment, vaccination, and iron replacement.[1,2] Nanoparticles may extend the half-life of delivered drug,[3,4] avoid drug degradation,[5] and modulate uptake into antigen-presenting[6,7] or other target cells.[8–10] The bio-physicochemical characteristics of drug delivery systems, viz. size, charge, surface behavior and composition of the polymer are conventionally considered, as these key factors impact on particle biodistribution. Although all aforementioned characteristics have been optimized to circumvent the rapid clearance by the mononuclear phagocyte system (MPS) in the spleen and liver,[3] in vivo results frequently fail to meet the expectation.[3] Thus, there is a need to refine this flaw, for instance by means of the geometry aspect.

Classically, particle shape has been disregarded as a feature, which may switch the biodistribution and circulation half-life. Sundry manufacturing methods, such as mechanical stretching,[6,11–13] lithography,[14–16] nonwetting templates,[17]

ADVANCED
SCIENCE NEWS
www.advancedsciencenews.com

ADVANCED
HEALTHCARE
MATERIALS
www.advhealthmat.de

and microfluidics,[18] enable the preparation of nonspherical nanoparticles and entitle the further investigation of particle geometry's influence on biological half-life and fate. It has been demonstrated that (prolate) ellipsoid particles display a lower internalization by macrophages.[8,19,20] In contrast, other geometries like discs (oblate ellipsoid) induce phagocytosis.[21] Ellipsoid particles also permit better antigen delivery to T cells.[9,22] These findings indicate that particle shape can be an eminent element affecting the fate of particulate drug delivery systems. However, the stability of nanoparticle shapes is still not much studied for biodegradable–biocompatible particles.

Therefore, the aim of this study is to comprehensively examine the correlation between nonspherical biodegradable nanoparticle shape stability and the physicochemical properties factors behind it, in physiological-related condition (37 °C, phosphate buffer saline (PBS) pH 7.4 310 mOsm). The film-stretching method was employed under dry heat to produce nonspherical nanoparticles from the spherical ones. The spherical nanoparticles were prepared by diverse fabrication methods (a. cross-linking: physical & chemical; b. molecular entanglement: emulsion solvent extraction & nanoprecipitation) and biodegradable materials (O-carboxymethyl chitosan [O-CMCHS], gelatin, carboxyl-ended poly(D,L-lactic acid) [PLA-COOH], and poly(D,L-lactic-*co*-glycolic acid) [PLGA-COOH]). In addition, we benchmarked the results to the common model, but less biodegradable nanoparticles (carboxylated poly(styrene) [PS-COOH] and silica [SiO$_2$] nanoparticles). In principle, several determining factors related to the nanoparticle shape stability have been elucidated and suggest that they strongly affect each other. In fact, the significant extent of residual stabilizers, which existed on nanoparticles, exhibited the best stability in terms of nonsphericity. We also discuss thoroughly this underlying issue and its potential implications for drug delivery and targeting.

2. Results

All spherical nanoparticles as a base of nonspherical nanoparticles were prepared in the similar hydrodynamic size (**Table 1**). Subsequently, the stretching in one direction with a stretching factor of 3 was performed toward spherical samples embedded in a poly(vinyl alcohol) (PVA) (Mowiol 40–88; bulk $T_g \approx 85$ °C[23]) film using a custom built device (**Figure 1**a) at certain stretching condition for different materials (Table S1, Supporting Information; see also Methods in Supporting Information for further details of particles embedment in the PVA film). The characteristics of resulted nonspherical (quasi prolate/elongated) nanoparticles after the standardized washing steps (see Methods in Supporting Information) are depicted in Table 1 and Figure 1b,c. The increase of hydrodynamic size and polydispersity index (PDI) was clearly observed on nonspherical nanoparticles, whereas zeta potential exhibited practically no change.

2.1. Effect of Fabrication Method

First, the comparison between two fabrication methods (cross-linking vs molecular entanglement) was performed. Because of the stabilizer/surfactant absence in the cross-linking

Bernard Manuel Haryadi, a grantee of DAAD Research Scholarship, is recently pursuing his Ph.D. at the Ludwig-Maximilians-Universität München under the supervision of Prof. Gerhard Winter and Prof. Julia Engert. His research interests encompass: a) advancement of smart-biomaterials for nanomedicine; b) anisotropy on particles intended for drug delivery and targeting; c) therapeutic protein–peptide formulation; d) pharmaceutical unit process development; e) biomolecular corona; and f) molecular modeling computer simulations of material behaviors at nano–bio interfaces.

Gerhard Winter obtained his Ph.D. degree in pharmaceutical technology at the University of Heidelberg, Germany, under the supervision of Prof. Herbert Stricker in the area of transdermal absorption simulations in 1987 with summa cum laude distinction. He has an around 10 year career in pharmaceutical industries (Merck, Boehringer, and Roche, chronologically) as a laboratory head, thus excels in numerous unit operation processes, development steps, and dosage forms. In 1999, he was appointed as a full professor for Pharmaceutical Technology and Biopharmaceutics, Center for Drug Research at the Ludwig-Maximilians-Universität München, Germany. His research interests include protein stabilization, parenteral dosage form technology, novel drying technologies, drug delivery systems, and colloidal drug formulations.

Julia Engert is a private lecturer in the group of Prof. Gerhard Winter, Department of Pharmacy, Ludwig-Maximilians-Universität München, Germany. She completed her Ph.D. studies supported by the University of Otago Postgraduate Scholarship at the University of Otago, New Zealand, in 2008, under the supervision of Prof. Sarah Hook and Prof. Thomas Rades, in pharmaceutical technology. Her research interests include the assessment of specific aspects of both desired (e.g., vaccination) and undesired (e.g., aggregates) immunogenicity of protein pharmaceuticals, needle-free vaccination techniques, and nano- and microparticulate delivery, including the preparation and investigation of nonspherical particles. She currently works at the Regional Office for Health and Social Affairs Berlin (LAGeSo) as inspector for good manufacturing practice (GMP) and good clinical practice (GCP) in the Pharmaceutical Inspectorate.

Table 1. Characteristics of spherical and nonspherical nanoparticles used in the study (Data are expressed as mean ± standard deviation ($n = 3$)).

No.	Polymer	Preparation method	Involvement of stabilizer	Hydrodynamic size, S_h [nm]		Polydispersity index PDI		Zeta potential [mV]		Yield [%]
				Spherical	Nonspherical	Spherical	Nonspherical	Spherical	Nonspherical	
1	PLA-COOH	Nanoprecipitation	No	179.3 ± 4.1	404.5 ± 17.8	0.055 ± 0.043	0.215 ± 0.096	−14.2 ± 0.6	−15.5 ± 1.7	96.2 ± 3.2
		Emulsion solvent extraction	Yes (PVA)	175.1 ± 3.3	413.7 ± 20.4	0.043 ± 0.033	0.213 ± 0.028	−7.6 ± 1.4	−8.2 ± 2.3	80.6 ± 2.1
			Yes (P407)	180.8 ± 0.6	419.3 ± 9.9	0.055 ± 0.023	0.254 ± 0.027	−9.6 ± 2.3	−8.4 ± 1.5	75.5 ± 2.3
			Yes (TPGS)	153.5 ± 2.6	410.0 ± 14.1	0.134 ± 0.029	0.194 ± 0.019	−11.5 ± 0.9	−10.9 ± 1.2	72.1 ± 2.0
2	PLGA 75/25-COOH	Nanoprecipitation	No	172.3 ± 3.8	390.6 ± 6.9	0.081 ± 0.010	0.273 ± 0.023	−13.4 ± 2.3	−14.1 ± 0.5	95.7 ± 3.9
		Emulsion solvent extraction	Yes (PVA)	168.1 ± 0.8	430.3 ± 13.4	0.029 ± 0.028	0.223 ± 0.025	−8.5 ± 1.7	−7.6 ± 0.6	81.1 ± 0.8
3	PLGA 50/50-COOH	Nanoprecipitation	No	176.6 ± 0.9	346.8 ± 6.6	0.022 ± 0.015	0.157 ± 0.063	−12.6 ± 1.2	−11.5 ± 1.0	63.8 ± 1.5
4	O-CMCHS	Ionic gelation	No	167.6 ± 0.8	382.6 ± 7.3	0.168 ± 0.007	0.145 ± 0.047	−11.4 ± 0.6	−3.7 ± -0.3	35.2 ± 0.2
5	Gelatin	One-step desolvation	No	188.1 ± 1.5	1007.0 ± 173.9	0.053 ± 0.009	0.632 ± 0.234	−16.6 ± 1.0	−2.0 ± 0.3	81.4 ± 0.3
6	PS-COOH	Emulsion polymerization	Yes (sulfate ester derivative)	178.8 ± 3.0	341.4 ± 9.7	0.032 ± 0.022	0.191 ± 0.031	−30.3 ± 0.8	−17.2 ± 0.3	N/A[a]
7	SiO₂ (AR3)	Polymerization	Yes (CTAB)	N/A[a]	255.5 ± 5.3	N/A[a]	0.228 ± 0.023	N/A[a]	−26.3 ± 1.5	88.3 ± 0.4[b]
8	SiO₂ (AR8)	Polymerization	Yes (CTAB)	N/A[a]	929.0 ± 16.2	N/A[a]	0.478 ± 0.023	N/A[a]	−22.9 ± 1.7	89.7 ± 0.2[b]

[a]N/A, not applicable; [b]Only these yields represent the direct (without film-stretching) processes in fabricating nonspherical nanoparticles. Other yields are based on the production of the spherical nanoparticles.

method, nanoprecipitation (no stabilizer/surfactant; also called solvent displacement[24,25] elsewhere) is the main focus in molecular entanglement development instead of methods involving stabilizer (e.g., emulsion solvent extraction; also called [emulsion] solvent diffusion[24,26] or [emulsion] solvent evaporation[2,24]) (Table 1).

The size of cross-linked hydrogel nanoparticles demonstrated by scanning electron micrographs (SEM) (Figure 1b) was measured in dry milieu (leading to significant particle shrinking), thus may be considerably different as reported by dynamic light scattering (DLS) in Table 1.[27] No significant shrinking of nanoparticles occurred on more solid nanoparticles composed from aliphatic polyesters via nanoprecipitation and commercial standard PS-COOH (Figure 1c). After three-times stretching from its initial length, both cross-linked hydrogel nanoparticles appeared to be slightly elongated with initial aspect ratio (defined as the proportion of length to width ellipsoid particle) of 1.62 ± 0.18 and 1.11 ± 0.09 for gelatin and O-CMCHS, consecutively. These aspect ratios were much lower compared to the theoretical calculation (Figure 1d and Supplemental Calculation, Supporting Information). In addition, considerable swelling was exhibited by both, mainly gelatin nanoparticles (Figure 1b).

Over time, an obvious discrepancy was noted between the shape stability of the nonspherical nanoparticles. These discrepancies were not equal for all particles, but were strongly affected by many factors, including the fabrication method. To allow better shape stability prediction and comparison between the tested samples, the typical shifting time ($t_{1/2}$) (expressed as the time needed for a half decrease of initial aspect ratio) was

calculated. In hours, both nonspherical cross-linked hydrogel particles became virtually spherical at 37 °C (aspect ratio = 1; figures not shown), with gelatin demonstrated slightly better shape stability (Figure 1e). Due to swelling and poor shape stability, gelatin and O-CMCHs are only used as references in elucidating the factors affecting shape transformation of nonspherical nanoparticles.

Meanwhile, nonspherical nanoparticles formulated by aliphatic polyesters (Table S2, Supporting Information) and nanoprecipitation method exhibited much higher $t_{1/2}$ at 37 °C (**Figures** 1e, **2**, and **3**a [left], b,c), with PLGA 50/50-COOH (≈44 kDa) being the inferior one with almost 6 d. Because of this, our further study with emulsion solvent extraction method (involving stabilizer) for aliphatic polyesters is only focused on PLA-COOH and PLGA 75/25-COOH. Besides, the recent indication to use low molecular weight of aliphatic polyesters (≈15 kDa) for drug delivery[28] due to the success in clinical study, reinforces our polymer choices. As expected, the $t_{1/2}$ of PLGA 75/25-COOH & PLA-COOH nanoparticles by nanoprecipitation were much greater at 5 °C (Figures 1e, 2b, and 3b).

Nonetheless, the shape stabilities of nonspherical PLGA 75/25-COOH and PLA-COOH nanoparticles formulated by nanoprecipitation were still much poorer than the commercial standard PS-COOH prepared by emulsion polymerization (Figures 1e, 2, and 3b), i.e., approximately less than one-sixth at 37 °C and less than half at 5 °C. By applying emulsion polymerization in commercial standard PS-COOH, stabilizer was used during the preparation process and residual stabilizers may present in nanoparticles (Polysciences' Product Information).[29] To
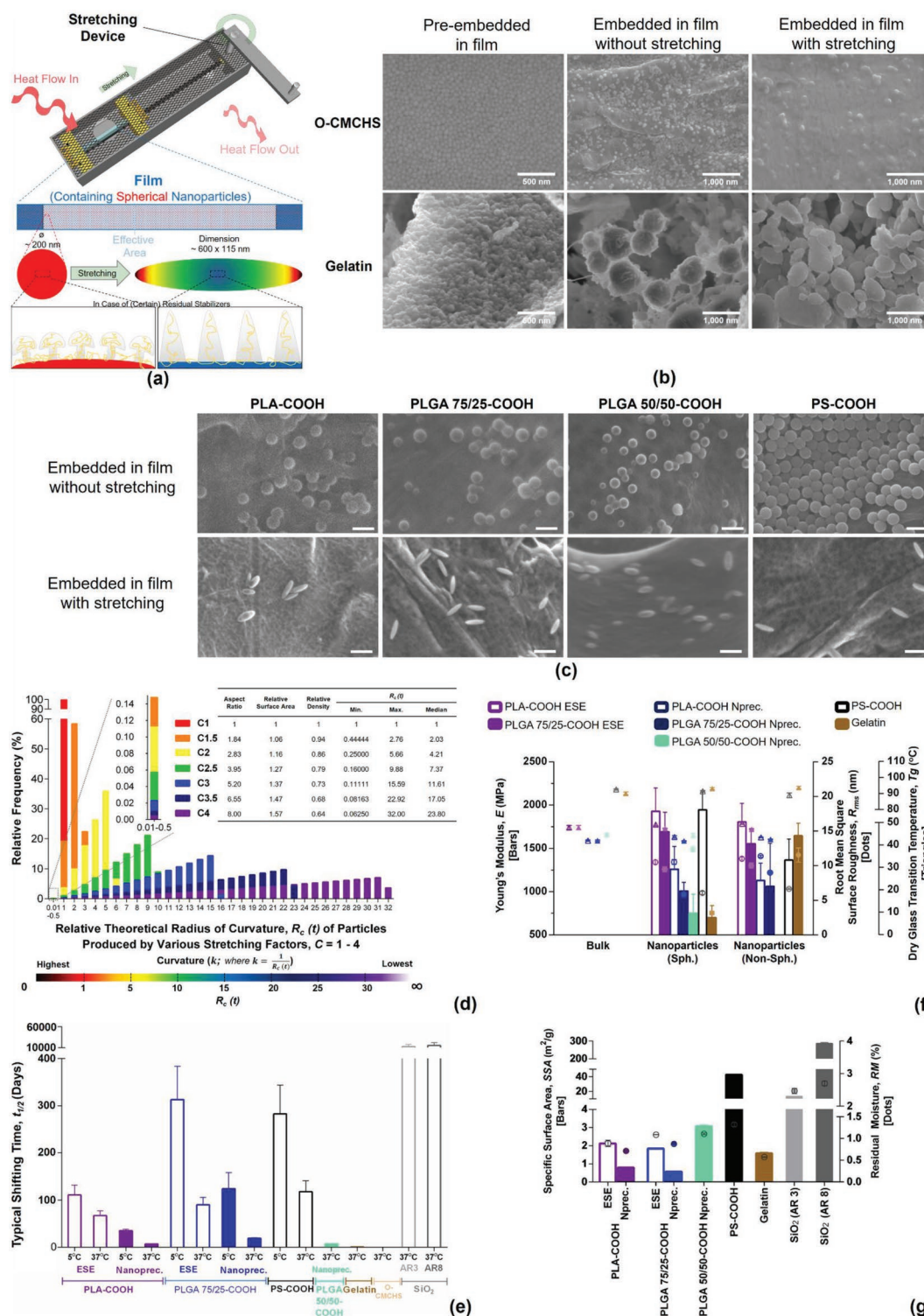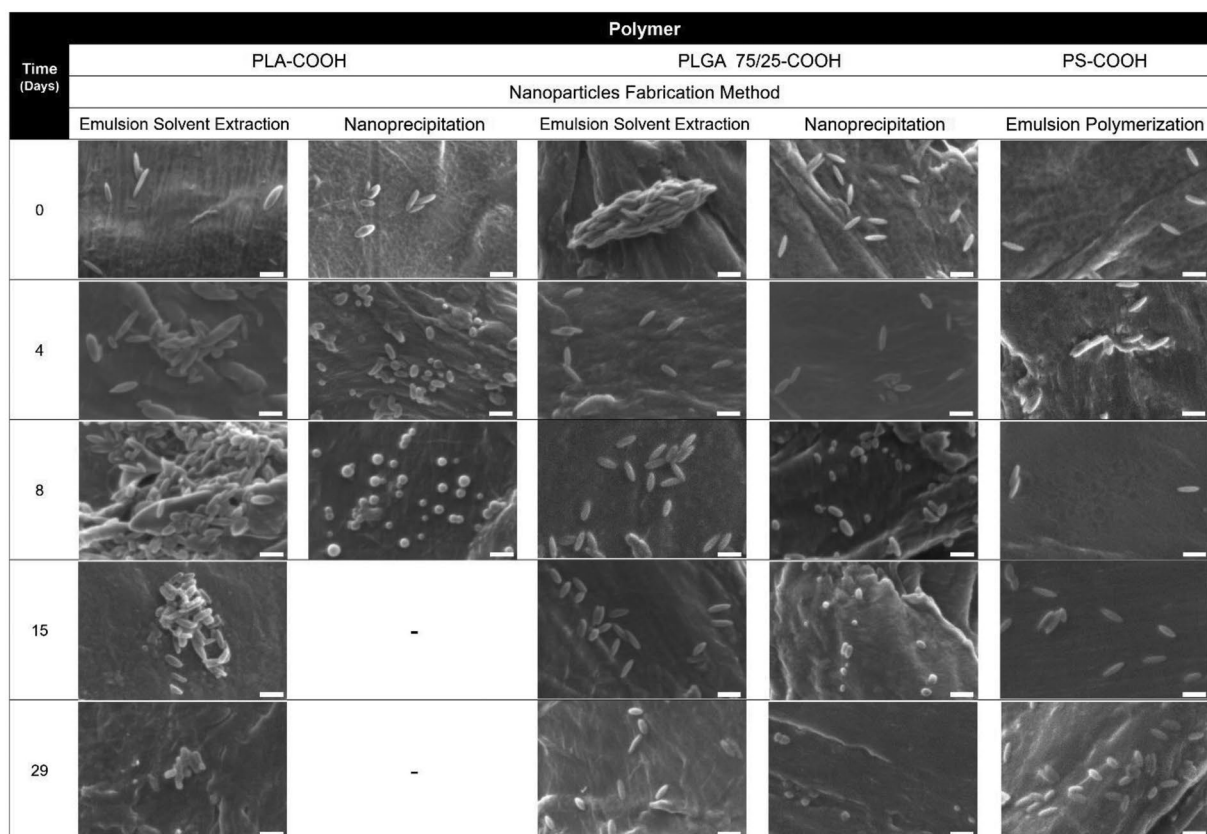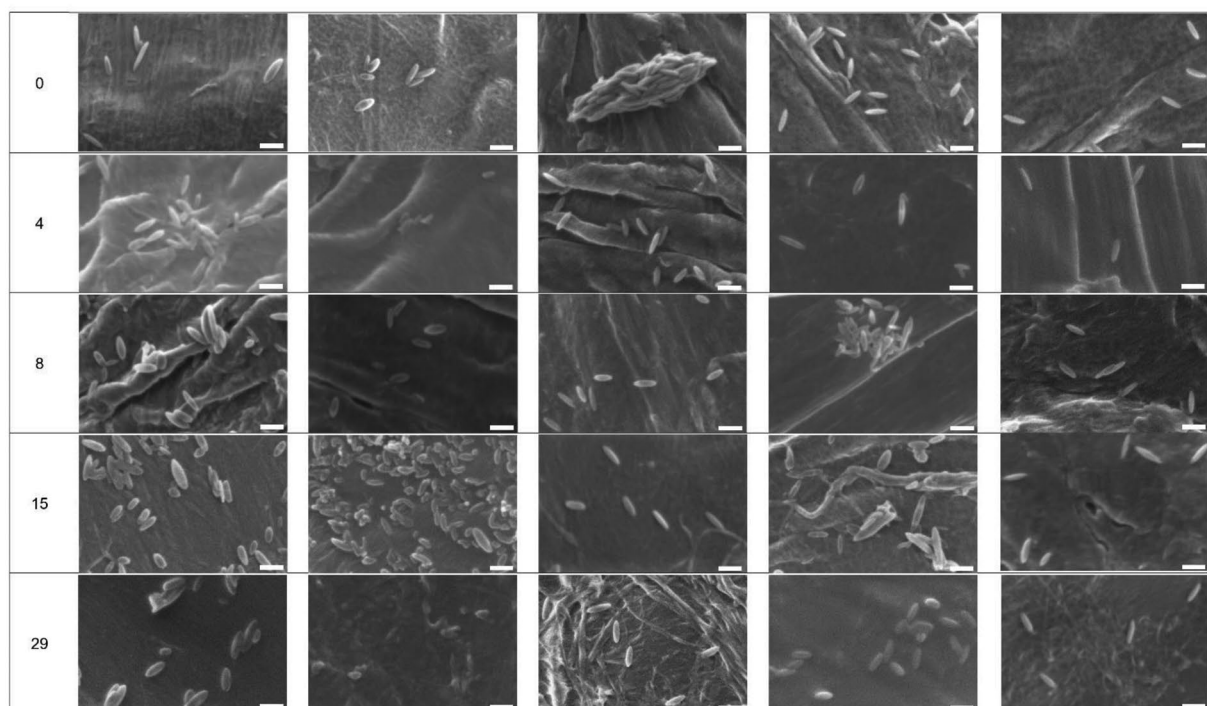
Figure 1. a) Schematic of film-stretching device utilized in this study for fabrication of nonspherical nanoparticles from spherical ones. It is also displayed the common and plausible architecture alteration of polymers at the nanoparticle interface after stretching,[187] involving the transition from "mushroom" to "brush" configuration. Scanning electron micrographs of spherical and nonspherical b) cross-linked hydrogel nanoparticles, encompassing O-CMCHS and gelatin, as well as c) aliphatic polyesters (prepared by nanoprecipitation) and PS-COOH nanoparticles (scale bars = 500 nm). For clarity, spherical nanoparticles of aliphatic polyesters and PS-COOH before their incorporation into film are not shown. d) Critical physical factors on prolate ellipsoid particle influenced by uniaxial stretching process. e) Calculation of typical shifting time ($t_{1/2}$) from aspect ratio (AR) of particles. f) Physiosorption-based surface characteristics of various evaluated nanoparticles. g) Mechanical properties of tested nanoparticles. Unless otherwise specified in Methods in Supporting Information, data represents mean ± standard deviation ($n = 3$).

ADVANCED
SCIENCE NEWS

www.advancedsciencenews.com

ADVANCED
HEALTHCARE
MATERIALS

www.advhealthmat.de

Figure 2. Representative scanning electron micrographs obtained on different days after initial preparation displaying shape stability of nonspherical aliphatic polyesters (PLA-COOH & PLGA 75/25-COOH) and PS-COOH nanoparticles. Nanoparticles were dispersed in phosphate buffer saline (PBS) pH 7.4 310 mOsm for a maximum of 29 d at a) 37 °C and b) 5 °C. Scale bars = 500 nm.
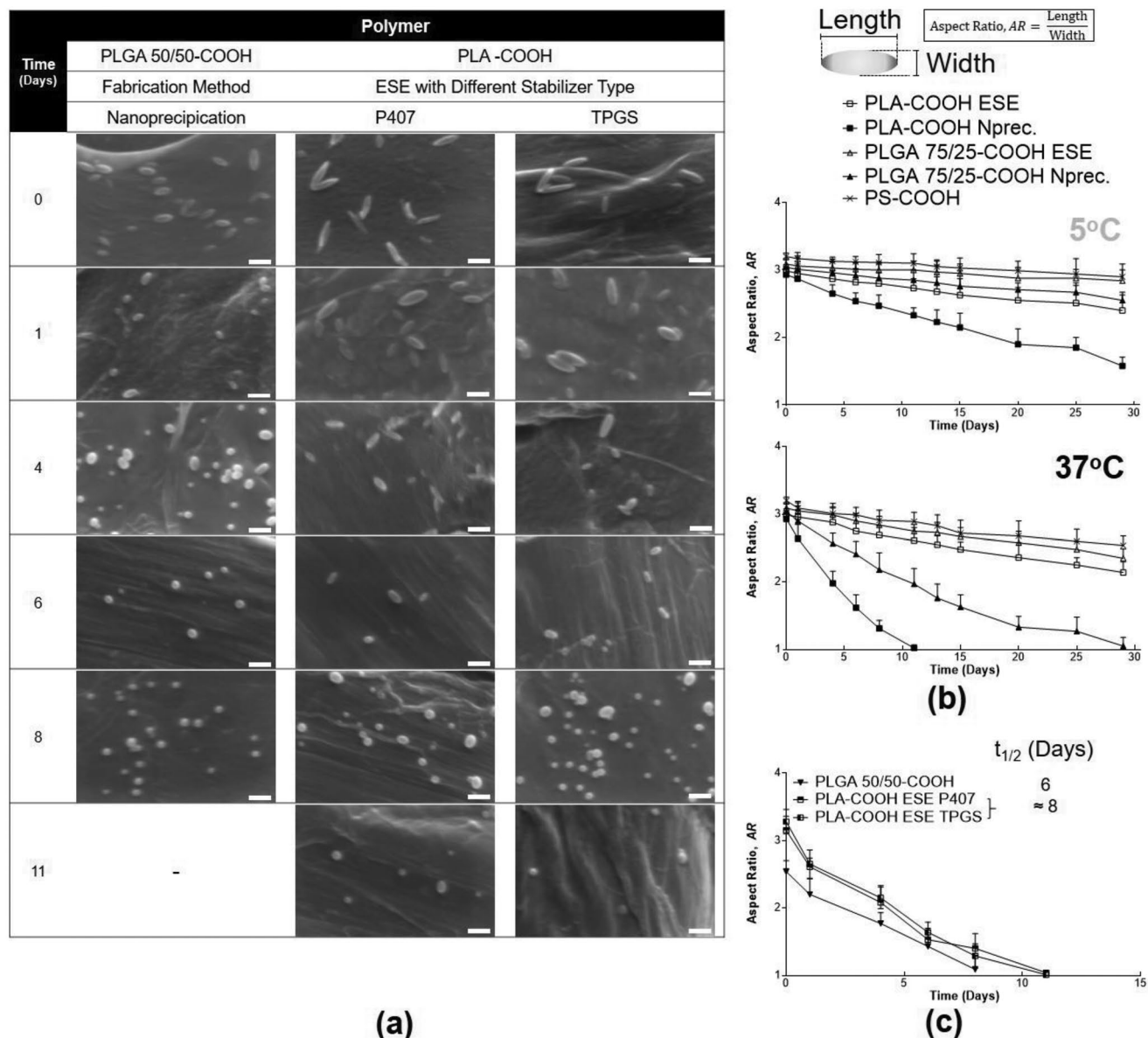
1900352 (5 of 31)

Figure 3. a) Scanning electron micrographs obtained on different days after initial preparation displaying shape stability of PLGA 50/50-COOH nanoparticles (formulated by nanoprecipitation) and PLA-COOH nanoparticles (manufactured by emulsion solvent extraction (ESE) technique with the variation of utilized stabilizers; in this figure, Poloxamer 407 denoted "P407" and TPGS are evaluated instead of PVA used in Figure 2). Scale bars = 500 nm. b,c) Plots of aspect ratio (AR) over time of aliphatic polyester prepared by different fabrication methods and PS-COOH nanoparticles at 5 °C and 37 °C. Figure 3b corresponds to the micrograph results from Figure 2a,b, meanwhile Figure 3c was derived from the measurement results of Figure 3a. Aspect ratio (AR) is calculated as described in the top of Figure 3b.

also permit stabilizer contribution in aliphatic polyester nanoparticles, an emulsion solvent extraction method with different stabilizers was employed. PVA (Mowiol 4–88), a semicrystalline polymer, elicited dramatic improvement of nonspherical shape stability for PLA-COOH and PLGA 75/25-COOH, both at 37 and 5 °C (Figures 1e, 2, and 3b). At 37 °C, the $t_{1/2}$ was enhanced up to about 11 times for PLA-COOH and fivefolds for PLGA 75/25-COOH. Other stabilizers a) Poloxamer 407 (P407) and b) D-α-tocopherol polyethylene glycol 1000 succinate (TPGS) were also evaluated in the fabrication of nonspherical PLA-COOH by emulsion solvent extraction. However, they failed to increase the

non-spherical shape stability of PLA-COOH (Figure 3a,c). No considerable $t_{1/2}$ alteration was observed between nanoparticles manufactured by emulsion solvent extraction using these stabilizers compared to the nanoprecipitation at 37 °C, i.e., between 6 and 8 d (Figure 3a,c). In this part, it can be summarized that for biodegradable polymers, PLGA 75/25-COOH prepared by emulsion solvent extraction using PVA is the longest-lasting aliphatic polyester in terms of nonsphericity. It is characterized by $t_{1/2}$ at 5 °C for almost 1 year and at 37 °C for roughly 3 months (Figure 1e). For this reason, PVA is chosen as the main discussion and stabilizer evaluated further in this report.

ADVANCED
SCIENCE NEWS
www.advancedsciencenews.com

ADVANCED
HEALTHCARE
MATERIALS
www.advhealthmat.de

Beside aspect ratio reduction, the inclinations to be spherical ultimately at 37 °C for nonspherical nanoparticles synthesized by film-stretching method were also supported by the results of hydrodynamic size measurement and PDI by DLS (**Figure 4**). DLS detected a gradual decrease of both parameters. There was no significant change of zeta potential and pH for all nanoparticles

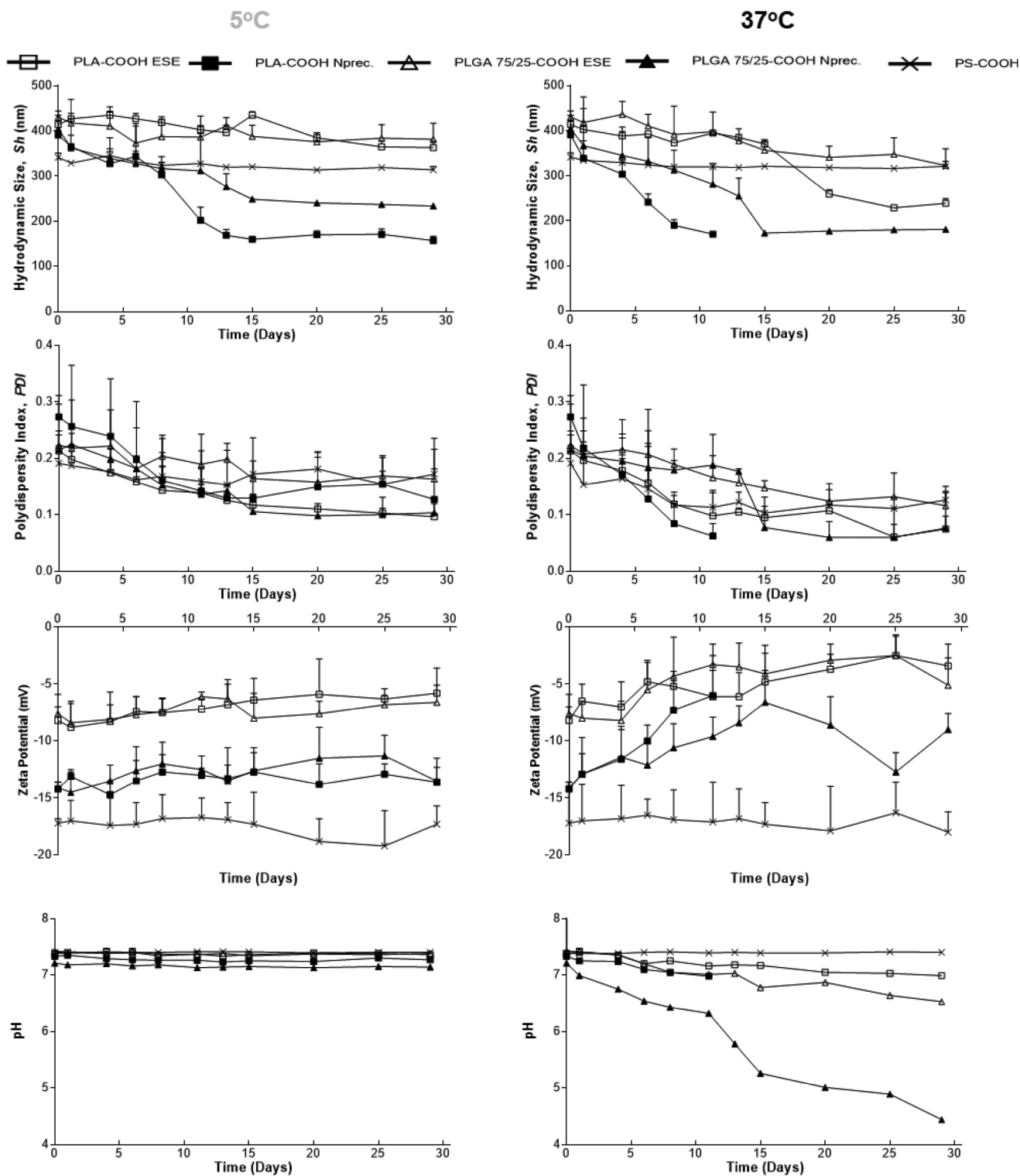**Figure 4.** Plots of hydrodynamic size, polydispersity index/PDI, zeta potential, and final preparation pH of low molecular weight aliphatic polyesters (PLA-COOH & PLGA 75/25-COOH) and PS-COOH nanoparticles over time. Aliphatic polyesters were prepared by different fabrication methods: emulsion solvent extraction (ESE) using PVA and nanoprecipitation. The data and time points in this figure correspond to Figures 2 and 3b.

stored at 5 °C, but substantial alteration of zeta potential and pH toward more acidic environment was observed at 37 °C on both aliphatic polyester nanoparticles (Figure 4). Meanwhile, PS-COOH nanoparticles exhibited practically no change of zeta potential and pH during observation (Figure 4).

To elaborate the causal factor of nonspherical shape instability on nanoparticles, the other factors (mechanical properties, porosity and hydrophobicity) are studied on selected nanoparticles and their data is displayed in the next sections.

2.2. Effect of Mechanical Properties: Young's Modulus, Surface Roughness (R_{rms}), and T_g

All nanoparticles were initially analyzed for mechanical properties in dry condition. Using atomic force microscope (AFM), it was revealed that they had relatively smooth surfaces, demonstrated by R_{rms} (**Figures** 1f and 5a) about tens nm or less,[30,31] and proportional Young's modulus to their bulk and the similar particles reported elsewhere.[23,32–34] Spherical gelatin and spherical PLGA 50/50-COOH nanoparticles (via nanoprecipitation) showed the smoothest and roughest surface (R_{rms} = 3.2 vs 12.4 nm). As expected, cross-linked system is rather smooth.[35] Regarding the Young's modulus, the softest and stiffest nanoparticles belong to gelatin (≈0.7 GPa) and PS-COOH (≈2 GPa) nanoparticles. Meanwhile, the T_g trends of (spherical) nanoparticles were: a) slightly lower than the bulk for aliphatic polyesters via nanoprecipitation and PS-COOH, and b) slightly higher than the bulk for aliphatic polyesters via emulsion solvent extraction and gelatin (Figure 1f).

After stretching, there were no considerable Young's modulus, surface roughness, and T_g differences of dry nanoparticles (prepared by lyophilization protocol; Figure S1, Supporting Information). The exception were: (a) gelatin nanoparticles obtaining greater Young's modulus and surface roughness about twofolds and threefolds, respectively, as well as b) PS-COOH and aliphatic polyesters, experiencing T_g reduction around 3 °C (Figure 1f). Nevertheless, there were clear trends that Young's moduli of stretched (nonspherical) aliphatic polyesters were: a) slightly lower for nanoparticles prepared by nanoprecipitation (possibly due to Young's modulus confinement effect[36]) and b) slightly higher for nanoparticles formed via emulsion solvent extraction utilizing PVA (Figure 1f). Besides, all stretched nanoparticles roughened after stretching, as depicted by greater R_{rms} (Figure 1f) and rougher sample surface profiles (Figure 5b vs a). The poststretching roughening effect is similar as commonly reported in micro-macroscale objects and various polymers.[37,38]

Surprisingly, it was revealed from the AFM results that between nanoparticles fabricated by nanoprecipitation, the spherical PLGA 50/50-COOH nanoparticles (the least-stable ones in terms of nonsphericity) have greater roughness (R_{rms} = 12.4 nm) compared to PLGA 75/25-COOH (R_{rms} = 5.9 nm) and PLA-COOH (R_{rms} = 9.5 nm). This result could be correlated with the porosity and hydrophobicity measurement, which are displayed and discussed in the subsequent sections.

To further confirm the marginal trend of T_g modulation of dry nanoparticles (dry T_g) compared to their bulk, the T_g of nanoparticles dispersed in aqueous medium (wet T_g) was also evaluated.

Only polymers that could be successfully and proportionally stretched into nonspherical nanoparticles were studied, namely aliphatic polyesters and PS-COOH. None of aliphatic polyester nanoparticles (initial ø ≈ 200 nm), however, exhibited a wet T_{gs}. It was very probable that their wet T_{gs} were superimposed by large endothermic peak of aqueous ice melting process (data not shown). It was reported[39,40] that even in macroscopic scale, aliphatic polyesters exhibited T_g reduction up to ≈10–20 °C, when they were contacted with high humidity (e.g., 90%RH) or water for 1 h or more. The longer the contact time with humidity or water, the greater the T_g depreciation. On the other hand, PS-COOH nanoparticles (initial ø ≈ 200 nm) showed more distinct T_g reduction, i.e., about 15 °C, compared to the dry ones (3 °C) (Figures 5c vs 1f). To study deeper the size dependence of T_g of polymers under soft confinement (nanoparticles dispersed in aqueous medium), other diameters of PS-COOH nanoparticles (100 and 2000 nm) were measured. The wet T_g of the PS-COOH nanoparticles lessen as the hydrodynamic size was reduced from 2000 to 100 nm, and thus the disparity against their bulk T_g grew considerably with smaller hydrodynamic size (1 vs 39 °C, respectively) (Figures 5c vs 1f). Similar finding was reported elsewhere.[41] Moreover, heat capacity change (ΔCp) appeared to be lesser with smaller hydrodynamic size, which is consistent with the published results.[42,43] Both phenomena (the reduction of wet T_g and ΔC_p) seemed to occur remarkably on non-spherical PS-COOH, obtained by 3x stretching of spherical PS-COOH (initial ø ≈200 nm). This may be attributed to the smaller particle size (in width and height dimension) (Figure 5b vs a), existence of much lower radius of curvature ($R_c(t)$), and wide variance of $R_c(t)$ on nanoparticles (Figure 1d). Likewise, the greater T_g diminution as smaller (hereafter denoted T_g confinement effect) and more aspherical PS-COOH nanoparticles, it is also very reasonable to propose that the T_g confinement effect occurred in the case of other nanoparticle materials, including aliphatic polyesters. Not to mention, because all nanoparticles for shape stability study were dispersed in the physiologically relevant medium (PBS pH 7.4 310 mOsm), it was very likely that the stronger ΔCp reduction occurred. The salt presence was reported to diminish ΔCp of macromolecules significantly.[44] As a result, less energy (represented by temperature and interfacial tension) is required to increase the polymer chain mobility in nonspherical nanoparticles, thus leads to more dramatic shape changes towards spheres. The T_g confinement effect further delineates that lower temperature (i.e., 37 or 5 °C) may still induce the aspect ratio decrease on tested nonspherical nanoparticles, mainly aliphatic polyesters.

2.3. Effect of Porosity of Particles

To quantify the porosity and hydrophobicity of the nanoparticles, physiosorption-based methods (specific surface area (SSA) and residual moisture analysis) were performed (Figure 1g). The analyses were conducted on starting spherical nanoparticles to generate more reliable and directly comparable results due to no swelling and similar nanoparticle size. The SSA of biodegradable nanoparticles that were included in film-stretching process highly varied, depending on the nanoparticle integrity, molecular weight, and bulkiness of the polymer chain.
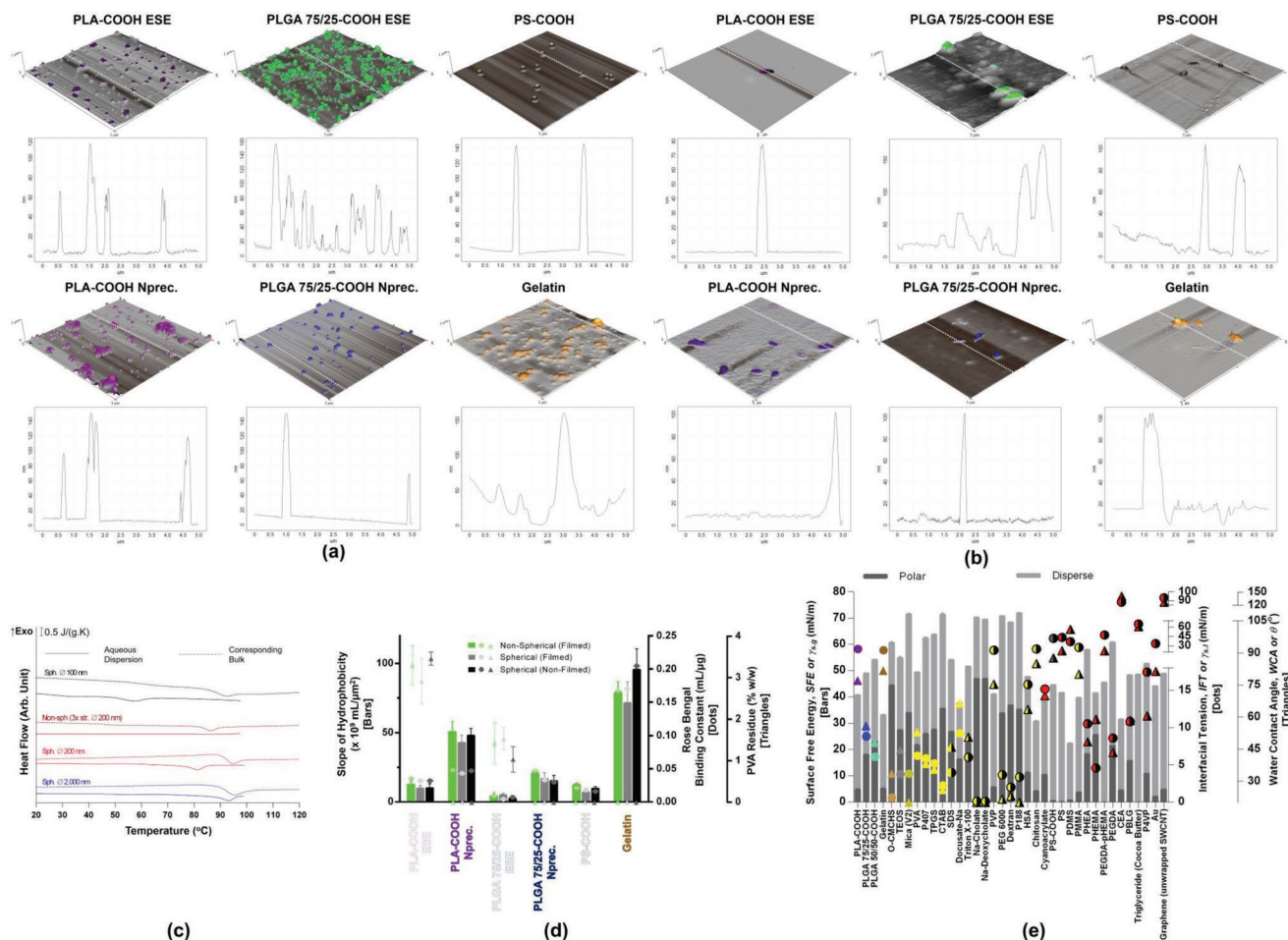
Figure 5. Atomic force microscope (AFM)'s 3D representations and surface or height profiles of evaluated a) spherical and b) nonspherical nanoparticles. c) Calorimetric thermograms of PS-COOH nanoparticles (solid lines), altogether with thermograms of their corresponding "bulk" polymer resulted from nanoparticles via annealing (dashed lines). These thermograms describe the dramatic disparity of nanoparticle T_g measured on dispersed or dry state. d) Nanoparticle's surface hydrophobicity (displayed by the slope of hydrophobicity and binding constant; the greater values mean greater hydrophobicity) and residual stabilizers (PVA) concentration profiles of tested nanoparticles. e) Correlation database of surface-free energy (SFE), material–water interfacial tension, and water contact angle (WCA) of various common materials functionalized as main component or excipient (e.g., stabilizer) in nanoparticle formulations. The used materials in our current nonspherical nanoparticle study are designated as points (either dot or triangle) without black borderline (and their corresponding bars), whereas points with black borderline (and their corresponding bars) show common materials for nonspherical nanoparticle fabrication used in other researches. The full points (and their corresponding bars) depict values generated from our measurement, while the half-filled points (and their corresponding bars) designate the recalculation values of interfacial activity parameters (using Owens and Wendt approach[223]) from references. Yellow (and their corresponding bars) represents our and commonly used stabilizers, while red (and their corresponding bars) is denoted as commonly reported materials in synthesizing biodegradable and/or nonspherical nanoparticles for drug delivery and targeting. Abbreviations and further details of referred material–nanoparticles: (1) SDS (sodium dodecyl sulfate),[168,224] (2) Docusate-Na,[168] (3) Triton X-100,[124,225] (4) Na-Cholate & -Deoxycholate,[129,226] (5) PVP (poly(vinylpyrrolidone)),[137,227] (6) PEG (poly(ethylene glycol))[209] 6000,[228] (7) Dextran,[194,228] (8) Poloxamer 188,[127,229] (9) HSA (human serum albumin),[134,230] (10) Chitosan,[98,178] (11) Cyanoacrylate,[98,231] (12) PS-COOH (carboxylated poly(styrene)),[4,232] (13) PS (poly(styrene)),[19,223] (14) PDMS (poy(dimethylsiloxane)),[83,223] (15) PMMA (poly(methyl methacrylate)),[83,223] (16) PHEA (poly(hydroxyethyl acrylate)),[71,73,233,234] (17) PHEMA (poly(hydroxyethyl methacrylate)),[233] (18) PEGDA (poly(ethylene glycol) diacrylate)[14–16,71,73,79,86,235]-PHEMA (poly(hydroxyethyl methacrylate)),[236] (19) CEA (2-carboxyethyl acrylate),[71,73,86] (20) PBLG (poly(γ-benzyl L-glutamate)),[142,237] (21) Triglyceride (cocoa butter),[115,116,160,163,164,238] (22) P4VP (poly(4-vinyl pyridine)),[149,150,239] (23) Au (gold),[220,240] and (24) SWCNT (single-walled carbon nanotubes).[46,241]

For instance, with respect to nanoparticles prepared without any stabilizer or surfactant, PLGA 50/50-COOH and gelatin nanoparticles were the least compact, displayed by SSA of around 3.05 and 1.57 m² g⁻¹, consecutively. For nanoparticles prepared by nanoprecipitation, again PLGA 50/50-COOH ("high" molecular weight [MW], bulkier) was the most porous or least compact, whereas PLGA 75/25-COOH ("low" MW, less bulky) had the lowest porosity or highest compactness (0.55 m² g⁻¹).

Furthermore, stabilizer had a strong effect on SSA, such as in emulsion solvent extraction for aliphatic polyesters, resulting about twofold SSA compared to the nanoprecipitation (Figure 1g). Overall, the nanoparticle material, having the highest porosity and produced to be nonspherical nanoparticles by stretching method, was PS-COOH (SSA ≈ 42 m² g⁻¹). We assume that the different amount of residual stabilizers may be one of the critical factors for the SSA differences between

ADVANCED
SCIENCE NEWS
www.advancedsciencenews.com

ADVANCED
HEALTHCARE
MATERIALS
www.advhealthmat.de

these groups. Our assumption was supported by quite diverse SSA value reported for aliphatic polyesters by emulsion solvent extraction (3–10 m^2 g^{-1})[45] and PS-COOH by emulsion polymerization (29 m^2 g^{-1})[46] nanoparticles. These reports used similar nanoparticle properties as reported here, namely diameter ≈200 nm, PDI < 0.1, and negative zeta potential of tens mV (for aliphatic polyesters).

Meanwhile, the residual moisture results appeared as a function of porosity (Figure 1g) and bulk-nanoparticle hydrophobicity (Figure 5d,e). In general, the higher the residual moisture, the greater the SSA, and the lesser hydrophobic the materials or nanoparticles. In other words, the presence of residual stabilizers may increase the SSA and residual moisture. Nonetheless, a large SSA did not negatively correlate to nonspherical nanoparticle shape stability, if the sufficient mechanical properties and appropriate hydrophobicity (indirectly encompassing residual stabilizers) were present.

2.4. Effect of Hydrophobicity of Materials and Particles

All nanoparticles (Figure 5d) were evaluated using the hydrophobic (log P 1.5[47]) anionic Rose Bengal dye method. Overall, the sequence of hydrophobicity between different nanoparticles (regardless of their shape) was as following (from the highest to the lowest): gelatin, PLA-COOH by nanoprecipitation, PLGA 75/25-COOH by nanoprecipitation, PLA-COOH by emulsion solvent extraction, PS-COOH, and PLGA 75/25-COOH by emulsion solvent extraction. This strong trend was inversely proportional with the nonspherical nanoparticle shape stability at 37 °C (Figure 1e), but poorly correlated to the bulk hydrophobicity (Figure 5e). Hence, the particle hydrophobicity study showed its importance.

No significant difference was found between initial spherical and film-embedded (without stretching) spherical nanoparticles in terms of nanoparticle hydrophobicity parameters, except for gelatin (Figure 5d). Unexpectedly, gelatin exhibited considerable lower hydrophobicity, ascribed presumably by strong adsorption of PVA (Mowiol 40-88 as the film matrix) onto gelatin nanoparticles. This adsorption may be responsible for the tangled thread-like structure around filmed and film-stretched gelatin nanoparticles in SEM and AFM (Figures 1b and 5b). As the further proof of PVA (semicrystalline polymer) presence, the hydrophilicity (Figure 5d), Young's modulus, and surface roughness (Figure 1f) of the nonspherical gelatin nanoparticles were greater compared to the initial spherical gelatin nanoparticles. This may be attributed to the typical properties of semicrystalline polymer after stretching,[48] namely demonstration of higher crystallinity. However, we could not measure the exact concentration of adsorbed PVA onto gelatin nanoparticles like to the aliphatic polyesters, due to the interference of adjacent hydroxyl (Figure S2, Supporting Information) in gelatin against colorimetric reagents in the reaction.[49]

As expected, the significant hydrophobicity reduction of PLA-COOH and PLGA 75/25-COOH nanoparticles fabricated by emulsion solvent extraction using PVA was strongly associated with its residue in nanoparticles, with the larger amount of PVA resided to PLA-COOH (the more hydrophobic polymer) compared to PLGA 75/25-COOH, namely about 3% versus 1.5%,

respectively (Figure 5d). Stronger PVA adsorption to the more hydrophobic materials aligns with established report.[50] Nonetheless, our results demonstrated that the intrinsic material hydrophobicity still played a dominant role in determining the nanoparticle hydrophobicity and nonspherical shape stability.

With regard to PS-COOH, we presumed that the superiority of nonspherical shape stability may also be aided by the presence of residual stabilizers utilized in the nanoparticle formation, beside by the relatively high dry bulk T_g of PS-COOH (i.e., ≈93 °C, which is still slightly higher than gelatin, ≈91 °C) (Figure 1f) and bulk[32]-nanoparticle Young's Modulus PS(-COOH) ≈2 GPa. This proposition is highly reinforced with the slightly poorer hydrophobicity data of bulk PS-COOH compared to gelatin (Figure 5e). The unsupportive situation (Figure 5e) encompassed the much lower polar component of surface-free energy (SFE) (or so-called surface polarity, X_p), water contact angle (WCA), and most important one: high material–water interfacial tension. We propose that the high material–water interfacial tension is the main, external, and rigorous driven force generating the biggest pressure on the tip of nonspherical nanoparticles (in other words, on the smallest $R_c(t)$ of nonspherical nanoparticles (Figure 1d) (Equation (1), adapted from Defay et al[51]). Consequently, the high interfacial tension leads to thermodynamically favorable spherical shape.

$$\Delta p = \frac{\gamma_{s.1}}{R_c(t)} \tag{1}$$

where Δp is the induced pressure, $\gamma_{s.1}$ is the solid–liquid interfacial tension (i.e., material–water) and $R_c(t)$ is the radius of curvature.

Hence, it is momentous to evaluate the suspected residual stabilizers in the starting PS-COOH nanoparticles (dispersed in highly purified water (HPW)), like PVA in the case of aliphatic polyesters by emulsion solvent extraction. First, using fast-acceptable sensitivity (i.e., energy-dispersive X-ray (EDX)) and routine (i.e., CHNS elemental or so-called oxygen combustion) analysis, it seemed that the PS-COOH nanoparticles were totally clean from the suspected sulfate ester derivatives (e.g., sodium dodecyl sulfate (SDS), docusate sodium, etc.). Using CHNS analysis, only C and H elements were detected with the ratio of 89.37% versus 7.62%, attributed likely to C and H from PS-COOH molecules. However, when the starting PS-COOH nanoparticles were measured in the instrument with a lower limit of detection, i.e., inductively coupled plasma atomic emission spectroscopy (ICP-AES), it evidenced 520 ± 70 ppm sulfur (S) and 100 ± 50 ppm sodium (Na), likely associated to the existence of residual stabilizers, which may bestow remarkable nonspherical PS-COOH nanoparticles shape stability.

2.5. Comparison to Nonspherical Silica (SiO$_2$) Nanoparticles

Because (mesoporous) nonspherical SiO$_2$ nanoparticles are subject of many publications ranging from the manufacture until in vivo study,[52–56] nonspherical SiO$_2$ nanoparticles were benchmarked to our nonspherical polymeric nanoparticles fabricated by film-stretching method. We synthesized two different aspect ratios (AR) of plain mesoporous nonspherical SiO$_2$ nanoparticles, namely ≈3 (simulating the similar aspect

ADVANCED
SCIENCE NEWS
www.advancedsciencenews.com

ADVANCED
HEALTHCARE
MATERIALS
www.advhealthmat.de

ratio and dimension with the stretched nanoparticles) and ≈8 (**Figure 6**). From the shape stability aspect, both nonspherical SiO$_2$ nanoparticles were excellent and superior against the most stable nonspherical PLGA 75/25-COOH manufactured by emulsion solvent extraction using PVA. The evidences were demonstrated by only slight diminution of aspect ratio, hydrodynamic size, and PDI after the storage in physiological-related condition for 29 d. The $t_{1/2}$ values are more than 10 000 and 13 000 d for aspect ratio 3 and 8, respectively (Figure 1e). The exceptional nonsphericity was in the same fashion as reported previously.[57] Simultaneously, zeta potential and pH of nonspherical SiO$_2$ nanoparticle preparation remained relatively stable (Figure 6).

Using the available instruments (i.e., differential scanning calorimeter (DSC) and thermogravimetric analysis (TGA)) and their working temperature range, neither liquefaction temperature (i.e., melting temperature (T_m)) nor other thermal events of nonspherical SiO$_2$ nanoparticles could be detected. It was reported, nonetheless, the T_m of bulk SiO$_2$ was 1600 °C.[58] Meanwhile, the Young's modulus (bulk) and surface roughness of bulk-mesoporous nanoparticle of SiO$_2$ were reported 73 GPa[59] and R_{rms} or R_a (average roughness) ≈2.5–10 nm,[60] respectively. The porosity and residual moisture of nonspherical SiO$_2$ nanoparticles for the aspect ratio 3 were ≈12.98 m^2 g^{-1} and 2.47%, whereas for the aspect ratio 8 were 285.6 m^2 g^{-1} and 2.70% (Figure 1g). These values may be interpreted that the mechanical properties (the prodigious liquefaction temperature and Young's Modulus, yet relatively smooth surface) and hydrophilicity of nonspherical SiO$_2$ nanoparticles successfully overpowered the impressive porosity in relation to elicit the tremendous nonspherical nanoparticle shape stability.

To further elucidate the hydrophobicity degree of SiO$_2$, the Rose Bengal method was applied. As expected, the hydrophobicity of SiO$_2$ (regardless of their aspect ratios) is much lower compared to the formerly tested polymers, characterized by virtually no Rose Bengal adsorption onto SiO$_2$ particles. Consequently, no graphic can be plotted like aliphatic polyesters, PS-COOH, and gelatin nanoparticles in Figure 5d. Furthermore, "SiO$_2$ bulk" (roughly represented by tetraethyl orthosilicate (TEOS), the monomer of SiO$_2$ nanoparticles]) also exhibited relatively low hydrophobicity, displayed by high SFE about 55 mN m^{-1}, low material–water interfacial tension ≈3.8 mN m^{-1} and WCA around 45° (Figure 5e). We suggest that both first parameters are better to be correlated with the nonspherical shape stability compared to merely WCA due to the absence of nonpolar or hydrophobic component consideration in WCA.

Likewise, residual stabilizer determination for PS-COOH nanoparticles, fast-acceptable methods (EDX and Fourier transform Infrared [FTIR]) were employed to both nonspherical SiO$_2$ nanoparticles. The results demonstrated that no bromide peak from cetyltrimethylammonium bromide (CTAB) and a carbon chain band (wavenumber 3000–2800 cm^{-1}) in the washed nonspherical SiO$_2$ nanoparticles (data not shown), implying that both nanoparticles might be entirely clean from residual surfactants. The similar results concerning the absence of Br after several washing steps of nonspherical mesoporous SiO$_2$ nanoparticle were reported formerly.[54] Nevertheless, it is plausible that the residual amount of CTAB is lower than limit of detection of the used technique. Therefore, oxygen combustion

method was performed and revealed that C, H, and N elements existed in both aspect ratios of SiO$_2$ nanoparticles with the ratio of about 1.00%, 3.12%, and 1.99%, respectively, but no Br was detected. To convince the residual CTAB in both nonspherical SiO$_2$ nanoparticles, Br analysis was performed using an inductively coupled plasma mass spectrometry (ICP-MS) and demonstrated that more than 96.8 ppb Br were detected.

3. Discussions

Here, the study for nonspherical nanoparticles fabrication covers the bottom-up methods, encompassing cross-linking (physical and chemical), molecular entanglement (nanoprecipitation and emulsion solvent extraction), and polymerization. We focus in these methods due to the potential thereof as the controlled release matrix. It is also possible to obtain nonspherical nanoparticles by diverse top-down methods (e.g., milling,[61] homogenization,[62] evaporative/antisolvent precipitation/solvent-diffusion[63,64]), but these approaches are commonly intended to enhance the dissolution of drug substances due to the greater surface area of nonspherical nanoparticles compared to the spherical ones with the same volume (or so-called: greater surface-to-volume ratio; Figure 1d).

Through the implementation of film-stretching method to the spherical nanoparticles (produced by the first two aforementioned bottom-up methods), it is basically believed that the shape-memory programming is introduced to the nanoparticles.[65,66] The spherical nanoparticles may be regarded as a primary shape. Subsequently, the primary shape is then mechanically deformed into a secondary shape at temperatures exceeding the bulk T_g (e.g., Table S1, Supporting Information vs Figure 1f). In this work, it was undergone merely uniaxially (however, it was also reported the plausibility of biaxial stretching,[4,33,67,68] imparting much higher aspect ratio, surface area, and variation of radius of curvature ($R_c(t)$), but very low density of particle constituents (Supplemental Calculation, Supporting Information) compared to the uniaxial one). Consequently, the sample is cooled below the bulk T_g, while still under stretching, to induce crystallization. Next, the secondary shape is preserved through an abrupt reduction in polymer chain mobility. Generally, the recovery to the primary shape in shape memory is then attained by simply heating the unconstrained network above dry bulk T_g. The resulting increment in polymer chain mobility permits the entropic energy lost during stretching to be converted into a restorative force that reestablishes the primary shape of the network. Nevertheless, we reported here that the recovery to the original state occurred below the bulk T_g (chiefly at physiologically relevant condition: 37 °C, PBS pH 7.4 310 mOsm), depending on the complex physicochemical parameters of bulk and fabricated nanoparticles.

In principle, it appears that by stretching or formation of nonspherical particles, the neater alignment of polymer chain arrangement in nanoparticle is formed. The higher order is, however, not favored thermodynamically. At higher temperature (e.g., 37 °C), the larger entropy is triggered, which may lead back the polymer chain to the preferable disorientation. The degree of polymer chain mobility, indicated by the rate of
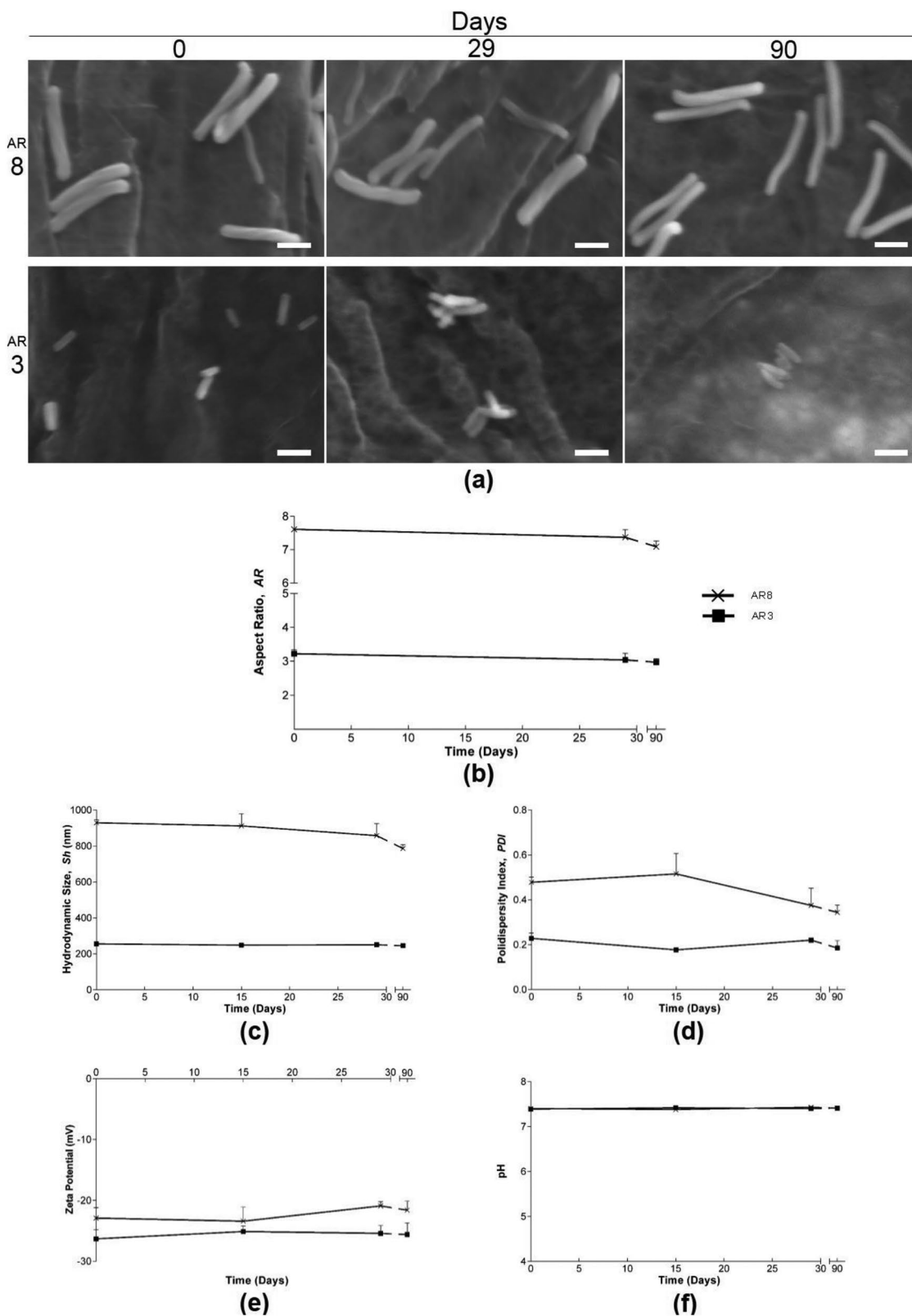
Figure 6. a) Scanning electron micrographs obtained on different days after initial preparation displaying shape stability of plain nonspherical mesoporous SiO_2 nanoparticles with the aspect ratio of ≈8 and ≈3. Nanoparticles were dispersed in phosphate buffer saline (PBS) pH 7.4 310 mOsm for a maximum of 90 d at 37 °C. Scale bars = 500 nm. Plots of b) aspect ratio (AR), c) hydrodynamic size, d) polydispersity index/PDI, e) zeta potential and f) final preparation pH of corresponding non-spherical mesoporous SiO_2 nanoparticles.

shape transformation into spheres in this report, is subject of multifarious physicochemical properties of bulk and fabricated nanoparticles (discussed in the following sections). On the contrary, as expected, nanoparticle storage at lower temperature (e.g., 5 °C) can aid to lessen the entropy level, thereby reduce dramatically the higher disorientation inclination of polymer chain arrangement. In other words, low storage temperature maintains longer the nonsphericity of nanoparticles.

3.1. Effect of Fabrication Method

3.1.1. Cross-Linking

In principle, the swelling of hydrogels (e.g., O-CMCHS and gelatin) at physiological pH (7.4) was very favorable, even for the highly (chemically) cross-linked hydrogel system as demonstrated elsewhere.[69] It is due to the existence of charge from the isoelectric point (IEP) of the polymers (i.e., IEP of O-CMCHS: 2.0-4.0;[69] gelatin type B: 4.7–5.4[58]) at physiological pH. We have tried to harvest both nonspherical cross-linked hydrogel nanoparticles from PVA (Mowiol 40-88) film using only HPW (pH 5.5–5.8) as well, however, the exaggerate swelling still occurred (similar appearances like in Figure 1b). The considerable swelling in the nonspherical cross-linked hydrogel nanoparticles by the film-stretching method may be explained by the facts that swelling is more pronounced in the cases of smaller submicron (i.e., size ≤ 200 nm), less cross-linked (for O-CMCHS), and heated particles.[16,70] From these findings, it can also be inferred that swelling is actually displayed by hydrogel particles prepared by any materials (e.g., poly(hydroxyethyl acrylate) /PHEA, poly(ethylene glycol) diacrylate /PEGDA,[70] derivatives of hydroxyl PEG acrylate groups,[71,72] etc.) and methods (i.e., imprint lithography, irrespective from its subtypes,[16,70] particle replication in nonwetting templates [PRINT],[71–76] etc.), but they are in the much lesser degree.

In our study, although the employed gelatin nanoparticles as prepared by Geh et al.[77] had been highly cross-linked (≈85%) using the standard chemical (covalent) cross-linker (i.e., glutaraldehyde), dramatic swelling thereof after embedment in PVA film matrix still took place (Figure 1b). This might be more associated with the heating history of gelatin nanoparticles in PVA film matrix (including its strong interaction with PVA as presented in the section "Results") as well as its small submicron size. Moreover, the strong interaction between hydrophobic part of gelatin and PVA was utilized to develop gelatin nanoparticles without crosslink.[78] The remarkable interaction may also occur between PVA and other hydrogel systems, such as lithography (e.g., S-FIL,[14] J-FIL,[15,79] and D-FIL[16]) or PRINT®[71–73,75] method.

Nonetheless, the stretched gelatin nanoparticles had a slightly (far from ideal; Figure 1d) nonspherical (prolate) shape, favorably associated with the immediate shape transformation during harvesting and storage in physiological-related condition. This might be explained merely due to the greater hydrophobicity of gelatin bulk materials (higher than other protein, such as human serum albumin (HSA); Figure 5e) and nanoparticles (as exhibited in section "Results"). It is because

in principle, the covalently cross-linked networks (like in gelatin nanoparticles) should show affine deformation toward stretching;[80] meaning it should behave likewise the thermoplastic polymers (e.g., aliphatic polyesters, polystyrene, etc.).[65] In the case of O-CMCHS owning the poorest nanoparticle nonsphericity, it may rather be ascribed to the lack of nanoparticle integrity, due to the consideration of its high bulk hydrophilicity (Figure 5e) and T_g (140–150 °C).[81]

Regardless of the poor results of nonspherical cross-linked hydrogel nanoparticle shape stability, we also suggest that because of the exaggerate swelling, film-stretching method seemed inappropriate for the production of nonspherical cross-linked hydrogel nanoparticles. Hence, this paper remonstrates the prior suggestion by Champion et al.[82] that the film-stretching method would be rather versatile for the nonspherical nanoparticles fabrication using various bulk materials and nanoparticles. Nevertheless, film-stretching method may be still appropriate for other (more solid) cross-linked particles (e.g., poly(methyl methacrylate) [PMMA][83]).

For the manufacturing of milder swollen nonspherical hydrogel micro- and nanoparticles (which usually have low [but tunable] Young's modulus[71–73]), imprint lithography or PRINT technology (a top-down method[84]) may provide more promising possibilities. However, certain component material(s) on both technologies are not biodegradable, e.g., PEGDA.[14,85] Furthermore, and importantly, we should be aware and critical to the potential instability of their nonspherical shape in relation to the comprehensive manufacturing aspects, mainly the hydrophobic degree of particle component materials (Figure 5e). Some of examples of these system are discussed below.

For the first instance, the synthesis of moderately hydrophobic nonspherical (biconcave or complex oblate ellipsoid) hydrogel microparticles has been demonstrated (with the details: particle Young's modulus $7.8–63.9 \times 10^{-6}$ GPa;[73] consisting of PHEA [≈up to 80% as main polymer], 2-carboxyethyl acrylate/CEA [10% as negative charge bearing agent], and PEGDA [1–10% as cross-linker; bulk Young's modulus: 0.01–3 GPa[86]]). By virtue of deliberation of their comprehensive manufacturing aspects (i.e., low Young's modulus, poor bulk T_g [likely <22 °C,[87] depending on the water content], and moderate hydrophobicity of their components and final preparation [which may be comparable to aliphatic polyesters; Figure 5e]), we believe that this system is favorably to encounter shape transformation into spheres in physiological-related condition, even the transformation rate is possibly slower than at the nanoscale.[26] But, there was no report regarding its nonspherical shape instability because they used 0.1% PVA (2 kDa) as dispersant that definitely stabilizes the shape of nonspherical microparticles (recall the case of our residual PVA results).

Second, PEGDA cross-linked by synthetic peptide (acrylated Gly–Phe–Leu–Gly–Lys/GFLGK) was employed to produce nonspherical hydrogel nanoparticles.[14] By using similar extensive approach as above, it is known that PEGDA nanoparticles have low, but tunable nanoparticle Young's modulus 0.255×10^{-6}–3 GPa[86] (depending on cross-link density), poor bulk T_g (≈-34 °C, regardless of its cross-link density[88]), T_g confinement effect, small $R_c(t)$, and mild-moderate hydrophobicity of their components. Based on these data, we propose that the nanoparticles may experience considerable nonspherical shape

ADVANCED
SCIENCE NEWS
www.advancedsciencenews.com

ADVANCED
HEALTHCARE
MATERIALS
www.advhealthmat.de

instability in physiological-related condition. Our proposal is strongly evinced by the very rapid transformation of similar nonspherical nanoparticles into spheres after the contact of (unconstrained) particles with HPW.[89] Therefore, the omission of supposedly high amount of stabilizer (PVA 31 kDa) postsynthesis process was performed.[14] From these two examples, it is noteworthy to point out that the presence of proper stabilizer exhibits the superior nonspherical particle shape stability.

Lately, instead of optimizing the commercially available stabilizer and materials for supporting the excellent nonspherical particle shape stability, it is not surprising that the trend in finding and utilizing less hydrophobic novel polymers as particle core grows significantly. The eminent examples thereof encompass the members of hydroxyl PEG acrylate (HPA) group,[71] such as triethylene glycol monoacrylate (TEGA),[72,75] and tetraethylene glycol monoacrylate (HP$_4$A).[74,76,90] Nevertheless, these new polymers have bulk T_g much lower than their parent polymer PEGDA,[91] where the hydrophobicity is inversely proportional to the length of hydrophilic side groups[91] (e.g., i.e., T_g TEGA -48 °C[91] vs T_g PEGDA -34 °C[88]). Therefore, it will be very fascinating to investigate the best compromise between the hydrophobicity aspects and the other physicochemical properties (e.g., T_g, Young's modulus, etc.).

3.1.2. Molecular Entanglement

To hinder excessive aggregation (principally during nanoprecipitation), the entanglement of polymer chain should be optimized by an appropriate polymer molecular weight. Relatively low molecular weight polymer is highly recommended,[92] such as ≈17 kDa (as used here). The larger molecular weight (≈44 kDa) of PLGA 50/50-COOH is still proper for nanoprecipitation process (which is in agreement as reported up to ≈61 kDa or 0.67 dL g^{-1} intrinsic viscosity[93]). However, the higher the polymer molecular weight by nanoprecipitation, the lower the nanoparticle yield due to the more aggregates formation (Table 1). The low-molecular-weight aliphatic polyester (17 kDa) might have surface active properties,[94] thereby permits better nanoparticle yield and integrity as well as compactness (low porosity). Therefore, it is not surprising that the higher porosity of aliphatic polyester nanoparticles (i.e., PLGA 50/50-COOH 0.67 dL g^{-1}) prepared by nanoprecipitation has been developed as "sponge" core for toxin entrapment.[95]

It is notorious that aliphatic polyesters[26,65] and PS(-COOH)[96] have shape-memory properties. For aliphatic polyesters, the shape-memory properties are more pronounced in the case of ester-ended variant, very low molecular weight (4.1 kDa) and very low bulk T_g (27 °C).[26] Whereas carboxyl-ended modification has better solubility in water and physiological pH, thus enables lower interfacial tension to the nanoparticles during their dispersion on these media. It is also known that the smaller the particle size (at the submicron or nanoscale), the higher possibility and rate of shape change.[26,96] This finding is associated with the larger impact of interfacial tension at the nanoscale[26,96] and lower $R_c(t)$ (Figure 1d). Even the shape shifting of pure macroscopic poly(styrene)/PS sheet ($R_c(t)$ ∞) was reported at a temperature below its bulk T_g, viz. 60 °C[97] versus 100 °C,[23] consecutively.

From the "Results" section, it is very clear that the involvement of particular stabilizer (only PVA [Mowiol 4-88] in the emulsion solvent extraction for PLA-COOH and PLGA 75/25-COOH; sulfate ester in the emulsion polymerization for PS-COOH; and CTAB in the condensation for SiO$_2$) might result the meaningful residual stabilizers albeit thorough and strictly standardized washing process, leading to much superior nonspherical nanoparticle shape stability in physiological-related condition. We believe and hypothesize that pure PS-COOH or PS nanoparticles (produced by surfactant-free process and in the same size range as tested here) may impart poorer nonspherical shape stability in physiological-related condition due to their higher bulk hydrophobicity than the carboxyl-ended aliphatic polyesters (Figure 5e). Likewise, we suggest that the nonspherical shape stability may also occur in the case of nonspherical core–(hydrophobic)shell systems having comparable or more inferior (e.g., T_g) physicochemical properties than materials tested here, such as cyanoacrylate–chitosan,[98] PLGA 15/85–chitosan,[8,99] and PMMA–(PS–PDMS)[83] (poly(methyl methacrylate);poly(styrene);poly(dimethylsiloxane)) (**Table 2** and Figure 5e). However, there was no implicit report regarding the particle shape stability thereof because of the dispersion unavailability in physiological-related condition (e.g., 5 °C,[98] high stabilizer content,[83,100] constrained in [unreleased from] rigid matrix,[89] or in organic liquid[83]), too short observation time (e.g., 1 h [8]), and particle storage only at dry and room temperature. According to our confirmative study, it is true that by storage of nonspherical aliphatic polyester nanoparticles at 25 °C (at ambient relative humidity) for 12 months in the constrained (unharvested) state in the PVA film, there was practically no aspect ratio decrease thereof (data not shown). To date, only few publications emphasize the plausibility of nonspherical particle shape transformation in physiological-related condition.[26,85]

3.1.3. Uncompromisable Requisite of Hydrophilic and Strongly Attached Stabilizer for Hydrophobic Bulk Nanoparticles

To preserve the nonsphericity of nanoparticles, it was known that in the PRINT system, 0.1–0.5% PVA (with very high interfacial activity due to the low degree of hydrolysis [75%] with 2, 20, or 22 kDa) is utilized intentionally as nanoparticle dispersant, including for in vivo study.[71–73,75,76,101] Instead of thorough washing, others also preferred to keep the high amount of PVA (2% 31 kDa[14]) or give extra Poloxamer (such as 0.75%[102] or 1%[103]) as dispersant in final preparation to endow better nanoparticle stability and circulation time. Importantly, some extra dispersants actually might not help much to stabilize the nanoparticles in the real physiological environment due to the rigorous dilution of the dispersant and if the stabilizer easily detaches from the nanoparticle surfaces.[104] Hence, the additional stabilizer postnanoparticle formation is mandatory for stabilizers that are weakly bound onto nanoparticles, such as Poloxamer 407[103] on aliphatic polyester nanoparticles;[105] otherwise the stabilizers were too inadequate to protect the nanoparticles from opsonization. In the case of our study, it is very reasonable that the P407 stabilizer is extracted by PVA used as the film matrix due to its strong retention to PVA.[106]

**ADVANCED
SCIENCE NEWS**

www.advancedsciencenews.com

**ADVANCED
HEALTHCARE
MATERIALS**

www.advhealthmat.de

Meanwhile, in case of TPGS, TPGS may have too low affinity (due to too hydrophilic) onto PLA-COOH nanoparticles, as reported elsewhere.[106,107] In-depth discussion of residual stabilizers is presented in the section "Discussion: Effect of Hydrophobicity of Materials & Particles."

3.2. Effect of Mechanical Properties: Young's Modulus, Surface Roughness (R_{rms}) and T_g

In principle, roughness (surface topography) correlates with the hydrophobicity (surface energy/surface chemistry) and wettability (WCA).[37] The impact of surface roughness may seem trivial, but our results showed its significance (recall the shape instability of rough nonspherical PLGA 50/50 by nanoprecipitation). Due to the necessity of sophisticated instrument for particle's roughness measurement (e.g., AFM), only a few papers have reported the influence of surface roughness to physiologically relevant phenomenon, e.g., protein adsorption[108] or so-called corona. This phenomenon gets more and more spotlights[109] because of its high correlation into clinical effect.[110,111]

Confinement effect was proved to be affected by the interfacial activities (in decreasing phase transition [including liquefaction] temperature of confined materials, irrespective of object geometry), existence of residual stabilizers, and kind of dispersion media.[41,112,113] Atoms at a free surface (such as in nanoparticles) encounter a diverse local milieu than do atoms in the bulk material. As a consequence, the energy related to these atoms will commonly be different from the atoms in the bulk. The additional energy linked with surface atoms is called SFE. In bulk materials, such SFE is characteristically ignored because it is attributed with merely a few layers of atoms near the surface and the ratio of the volume occupied by the surface atoms and the total volume of material of interest is low. Conversely, for smaller objects, the surface-to-volume ratio becomes very significant, and so does the effect of SFE.[36]

In general, macroscale objects have virtually no tendency to experience confinement effect compared to microscale[85,114] and nanoscale[36,42] objects. This trend may be ascribed to the higher surface-to-volume ratio of the nanoscale objects. Strong confinement effect on phase transition (e.g., liquefaction [T_g and T_m]) temperatures in nanoscale objects or radius of curvature does not only occur on polymeric systems (as reported here and elsewhere[41,42]), but also on any materials, both nonmetallic (e.g., water,[51] lipid,[115,116] etc.) and metallic ones (e.g., gold [Au],[117,118] lead [Pb],[119] tin [Sn],[119] bismuth [Bi],[119] etc.). Interestingly, it was reported that even in macroscale, certain polymer cases, such as bulk aliphatic polyesters, were also prone to the reduction of T_g due to absorption of nonfreezable water.[39,40] However, to our best knowledge, there is still no report discussing the relation between T_g confinement effect and nonspherical particle shape stability. Therefore, this report is the first one which proposes to correlate thereof. Nevertheless, it has been actually reported the shape evolution from the nonspherical to spherical nanoparticles on aliphatic polyester derivative (i.e., PEG block copolymer)–microparticles (initial Feret's diameter ≈ 50 μm)[85] and aliphatic polyester micro-nanoparticles (initial and final sphere ø 0.15–4 μm).[26] The PEG–aliphatic polyester block copolymer (having a lower bulk T_g than its native aliphatic polyester) was also described to encounter the T_g confinement effect.[120] Both reports used stabilizers during the nanoparticle formation, i.e., polysorbate (Tween) 20 (0.5%) during the washing step for the former and PVA (2%; molecular weight 10–30 kDa) during the solvent diffusion (also known as emulsion solvent extraction) process. The plausible rationale of residual stabilizers will be discussed deeper in the section "Results: Effect of Hydrophobicity of Materials & Particles."

For nanoprecipitation system (containing only aliphatic polyesters), the smaller Young's modulus and T_g are ascribed to merely confinement effect due to the smaller size (width and height) of nanoparticles and presence of very low $R_c(t)$ (Figure 1d). Meanwhile, in the emulsion solvent extraction containing significant residual PVA, the slightly higher of mechanical properties are designated to the PVA, which is semicrystalline[121,122] and gains higher crystallinity after stretching.[123] It was also obviously observed the slightly growth of formulation's T_g of nanoparticles containing residual PVA due to antiplasticization effect, as reported elsewhere.[124] As comparison, in case of the presence of amorphous and crystalline variants in a polymer (e.g., polyethylene terephtalate (PET)[125] or polypropylene (PP)[126]), polymer stretching generally increases T_g and Young's modulus several folds because of crystallinity enhancement.

In many cases, residual stabilizers can also be problematic due to the decline of particle's T_g in final preparation. Although some other common stabilizers (Poloxamer,[105,127] TPGS,[128] cholic acid in sodium salt form,[129] and polysorbate [Tween] 80[130]) are practically easy to be cleaned from particles, but in an adequate amount in the final preparation, they are reported to lessen the system T_g. The T_g reduction is well known as the presumable main reason of burst release in drug delivery.[131] In our formulation, the insignificant amount of resided Poloxamer 407 and TPGS is well represented as the insignificant changes of formulation T_g (data not shown). It was reported when acting as stabilizer, TPGS would distribute only on the particle surface and by washing up more than two times, the remaining TPGS on the surface could not be detected anymore by X-ray photoelectron spectroscopy (XPS).[132,133] This may be the proper explanation for the poor protection of TPGS for nonspherical PLA-COOH nanoparticles fabricated by emulsion solvent extraction. In contrary, the particular amount and type of PVA (possessing high interfacial activity) could adhere irreversibly on particles surface prepared by emulsion solvent extraction via molecular interpenetration and multilayer adsorption mechanism,[134] thus affects particle's physical properties (including drug release from nanoparticles) and cellular uptake.[135,136] Interestingly, with regard to the residual stabilizers, the affinity and extent of residual PVA, Poloxamer, and TPGS on aliphatic polyester nanoparticles prepared by emulsion solvent extraction can also be differentiated from the freeze-drying results in HPW and without additional cryoprotectant (our unpublished data; in preparation). Only PVA could elicit spontaneous redispersion and practically no aggregation, which can be assigned as the sufficient amount and strong adsorption of PVA on nanoparticles. The aggregation degree of nanoparticles synthesized by the aid of Poloxamer 407 and TPGS is

Table 2. Physicochemical contrast of nonspherical polymeric core–shell nanoparticles prepared by film-stretching method (PIBCA, poly(isobutylcyanoacrylate); PLGA, poly(D,L-lactic-co-glycolic acid); PMMA, poly(methyl methacrylate); PS, poly(styrene); PDMS, poly(dimethylsiloxane)).

Parameters	Example					
	1		2		3	
Component	Core	Shell	Core	Shell	Core	Shell
Material	Cyanoacrylate (PIBCA)	Chitosan (low viscosity)	PLGA 15/85 (Degradex from Phosphorex, Inc., Hopkinton, USA)	Chitosan	PMMA	PS–PDMS (block copolymer)
Reported in reference(s)	[98]		[8,99]		[83]	
Young's modulus [GPa]	≈0.002[242]	0.002–0.003[243]	N/A[a]	≈0.002[243]	≈3[23]	PS 3.2–3.4[23] PDMS 0.36–0.87[244]
T_g [°C]	Bulk 130[245]	Bulk ≈100–150[81]	Nanoparticle 40–41[8,99] Bulk N/A[a]	Bulk ≈100–150[81]	Bulk 106–113[23]	PS bulk 100[23] PDMS bulk ≈123–150[23]
Bulk hydrophobicity	Refer to Figure 5e	Refer to Figure 5e	–	Refer to Figure 5e	Refer to Figure 5e	Refer to Figure 5e
Positive remarks	• High bulk T_g (PIBCA & Chitosan) • Dry heat stretching procedure • Further information availability of chitosan properties		• High bulk T_g (Chitosan)		• Intermediate (PS) & high (PMMA < PDMS) bulk T_g • Intermediate (PDMS) & relatively high Young's modulus (PS & PMMA) • Dry heat stretching procedure • A little information availability of washing process & used polymer molecular weight	
Negative remarks	• High hydrophobicity (PIBCA slightly < chitosan slightly < gelatin) • Very low Young's modulus (PIBCA ≈ Chitosan)		• Very low bulk T_g & relatively lower Young's modulus of PLGA 15/85 (due to high glycolide percentage)[58] • Very low Young's modulus (Chitosan) • Low wet T_g (nanoparticles) • Oil bath during stretching (thus, involvement of additional potential contaminants & organic solvent)		• Great hydrophobicity (PMMA ≈< PS slightly < PDMS)	
Unknown information	• Residual stabilizer amount • Details of washing process (including washing & redispersion factor) • Details of PIBCA (e.g., molecular weight) • Nanoparticle integrity (~porosity ~residual moisture) • Surface roughness • Nanoparticle hydrophobicity		• Residual stabilizer amount • Details of washing process (including washing & redispersion factor) • Details of core-shell materials (e.g., molecular weight) • Nanoparticle integrity (~porosity ~residual moisture) • Surface roughness • Nanoparticle hydrophobicity		• Residual stabilizer amount • More about washing & redispersion factor • Nanoparticle integrity (~porosity ~residual moisture) • Surface roughness • Nanoparticle hydrophobicity	

[a]N/A, Not available.

as inferior as the nanoparticles prepared by nanoprecipitation (no stabilizer). These results are in agreement with previous publications using other materials and shapes of nanoparticles.[127,132,137] Based on the experimental results, we propose a systematic approach to better explain and predict the non-washability of particular stabilizers, as depicted in-depth in the section "Discussion: Effect of Hydrophobicity of Materials & Particles."

3.2.1. Reverse Proof of Complex Physicochemical Properties Interplays

First instance: Successful Stretching at the Temperature Below Bulk T_g Using Nanoparticles Composed of Low Young's Modulus, but High T_g Material: Palazzo et al.[98] interestingly reported

that the manufacture of nonspherical nanoparticles using film-stretching method uniaxially could be undergone far (≈50–100 °C) below the bulk T_g of the polymer (Table 2). To our best knowledge, only this paper reports the success of film-stretching method below the T_g.[138] Others[4,13,68,139] (including this report) always employ the temperature higher (normally ≈20–30 °C) than the bulk T_g, regardless of the used stretching medium (dry heating or oil bath) and nanoparticle materials. Moreover, Lu et al.[138] should perform the stretching ≈100 °C higher than the T_g due to their device limitation. Palazzo et al. works might be feasible because of the low Young's modulus of the used materials (cyanoacrylate: i.e., poly(isobutylcyanoacrylate) [PIBCA] & chitosan; both ≈0.002 GPa; Table 2). We do not believe the reason that T_g confinement effect could be applied to explain it, because our works convincingly showed the inability to stretch PS-COOH

**ADVANCED
SCIENCE NEWS**

www.advancedsciencenews.com

**ADVANCED
HEALTHCARE
MATERIALS**

www.advhealthmat.de

nanoparticles (the highest nanoparticle Young's modulus that can be stretched in our study: ≈2 GPa; Figure 1f), even at its bulk T_g (Figure S3, Supporting Information). Conversely, ours confirmed that T_g should vary in diverse medium, as reported elsewhere.[113]

Nevertheless, we still can infer that the obvious interplay presence between Young's modulus and T_g yielded the certain resistance for stretching process (Figure S3, Supporting Information). In this case, although bulk T_g of PS-COOH (≈93 °C; Figure 1g) is much lower than both bulk T_g in Palazzo's work (in-between ≈100–150 °C; Table 2), PS-COOH nanoparticles cannot be proportionally stretched as our standard stretching process at 120 °C (Figure 2). Moreover, stretching PS-COOH nanoparticles at its bulk T_g only generate lemon-like nanoparticles partially from total nanoparticle population (Figure S3, Supporting Information). Our generated shape resembles the nanoparticle shape produced by them. This shape might be attributed to the weak elastic deformation because of the high resistance from polymer chain mobility in nanoparticles. In addition, because of high bulk (cyanoacrylate and chitosan) hydrophobicity, high material–water interfacial tension may also induce the nanoparticle shape switch during harvesting in aqueous medium (Figure 5e).

Second Instance: Unsuccessful Stretching at the Temperature Far Above Bulk T_g Using Nanoparticles composed of High Young's Modulus, but Low T_g Material: Cauchois[140] reported his failure to stretch spherical poly(γ-benzyl-L-glutamate) (PBLG) nanoparticles using film-stretching method. PBLG, a rigid[141] liquid crystalline material, has an unique (helical) internal structure, thus may exhibit either spherical or elongated particles, depending on its variants.[142] It has rather high hydrophobicity (in-between PLA-COOH & PLGA 75/25-COOH; Figure 5e), bulk Young's modulus 34 GPa,[143] and T_g ≈ 19 °C.[144] He found out that even the stretching process was performed at the temperature (i.e., 150°) far above the bulk T_g, spherical PBLG nanoparticles were unsuccessful to be deformed into the elongated ones.[142] The hydrogen bond, which should take an account as the main driving force in transforming stretched particles,[12] seems work limitedly for soft material (<10 GPa[145]), such as PS and PMMA.[83] To sum up, the Young's modulus of particles appears also to be one of a critical factor (besides T_g) determining the success of film-stretching method.

Based on both instances, we can conclude that the unavoidable interplay between multiple factors (Young's modulus, T_g, and surface chemistry) determines the deformability degree of nanoparticles (in this section, it is characterized by the success degree of nonspherical nanoparticle formation by film-stretching method). We estimate that the deformability degree in the film-stretching method may favorably represent (but of course, still less a couple order of magnitude) the geometry sensitiveness of nonspherical nanoparticles in the real aqueous dispersion toward the interfacial tension. Therefore, these evidences reinforce our hypothesis that the complex interplay of manufacturing aspects may affect the nonspherical nanoparticle stability. We cannot only concern in one-two aspect(s) and neglect the others.

3.2.2. Correlation of Interfacial Phenomena towards Geometry and Internal Structure

Because of the interfacial tension, spherical particles (having no specific internal structure (like all experimented here using wide angle X-ray diffractometry, data not shown) or merely amorphous state in nature) are formed thermodynamically from nonspherical particles in order to minimize the contact area to water (recall the relative surface area comparison of the same volume objects, but different shape in Figure 1d and Supplemental Calculation, Supporting Information). This phenomenon arises from the energetic cost of forming a surface. Therefore, the SFE of the system is minimized when the particle shape is spherical. Besides, spherical state may permit polymer chain inside nanoparticles to have larger cohesive energy.[146,147] Meanwhile, the greater surface area of nonspherical state (and the contribution of very low $R_c(t)$) will introduce more pronounced interfacial tension eliciting higher pressure. Consequently, the pressure would play a dominant role in the enhancement of polymer chain mobility on the surface, leading to the particle shape shifting into spheres.[148] To summarize, here is the condensed hypothesized correlation: the higher the hydrophobicity of materials/nanoparticles, the higher the interfacial tension, the higher the pressure working on nanoparticle surface, the faster the shape transformation into spheres. In brief, there is a sturdy relation between surface chemistry (hydrophobicity) and nonspherical shape stability/existence, as long as no robust or rigid internal structure. Our hypothesis is described on the next following examples.

First, beside well-defined amorphous aliphatic polyesters and PS-COOH studied here, another best example for the aforementioned hypothesis is poly(4-vinyl pyridine) (P4VP), an amorphous and a weakly hydrophilic polymer (Figure 5e). Likewise the aliphatic polyesters, P4VP (grafted by PS) exhibits shape-memory properties depending on media pH.[149–151] In contrast to aliphatic polyesters, the P4VP hydrophobicity becomes lesser at pH lower than its pKa (5.5) and reaches maximum at higher pH.[149,151] Therefore, these findings are recently employed to produce a pH-sensitive block copolymer with polystyrene (PS-b-P4VP).[149,150] In accordance with our interfacial activity database (Figure 5e) and other aspects of P4VP (bulk Young's Modulus 4.05 GPa[152] and T_g 142 °C[23]) and PS, it may be plausible that the nonspherical/elongated (so-called pupa-like) particles made from PS-b-P4VP may demonstrate relaxation into the spherical ones in physiological-related condition.[149] Our suggestion relies on the report by Deng et al.[150] revealing three key points that also fully support our hypothesis: a) addition of higher amount PVA (0.1%; 13–23 kDa and 88% hydrolyzed) during the manufacturing is indispensable for the greater nanoparticle hydrophilicity and thus, abundance of nonspherical nanoparticles; b) weak elongated internal structure exhibited by PS-b-P4VP (each material component Young's modulus ≈<4 GPa) can only be demonstrated with the considerable amount of PVA; and c) higher hydrophobicity caused by the incorporation of hydrophobic gold (Au) ≈40% (Figure 5e; bulk Young's modulus ≈65 GPa[153] and T_m 1064°C[154]) results the plumper nanoparticles (decrease of aspect ratio).

Second, to give a diverse/contrary approach, the tunably amphiphilic (SFE ≈ 22–45 mN m^{-1})[155] poly(2-oxazoline) family

was demonstrated. The increase of nanoparticle hydrophobicity by the incorporation of hydrophobic drug (i.e., Docetaxel (log$P$ 2.4[156]) or Paclitaxel (log$P$ 3.24[156]) into the amphiphilic worm-like poly(2-oxazoline) micelles (or so-called "filomicelles;" bulk Young's modulus ≈2–20s × 10^{-6} GPa[157] and bulk T_g ≈ 80 °C[155])) is proven to trigger an immediate transformation of nonspherical nanoparticles into spherical nanoparticles.[158] The higher the hydrophobicity induced by the particular drug (i.e., Paclitaxel) and higher drug loading (leading to larger particle–water interfacial tension), the more spontaneous and entire the spherical shape switch. In contrary to our current results displaying the preferable transformation from nonspherical into spherical particles during storage, Schulz et al.[158,159] reported that their drug-loaded nanoparticles turned gradually from spherical into worm-like particles due to the release of hydrophobic drug from nanoparticles (up to ≈60% for 25 d). Their observation was conducted at room temperature (≈25 °C) and 37 °C[159] (far below the drug loaded-nanoparticle T_g 73–76 °C) and in physiological-related medium (phosphate buffer saline [PBS] pH 7.4 310 mOsm).

Third, for nanoparticles having its own definite internal structure, large interfacial tension because of high hydrophobicity or very low Young's modulus could be simply overcome. As a consequence, they may generate superior shape stability[142] or even, nonspherical nanoparticles spontaneously from the spheres over time.[115,160–163]

The former example is represented by PBLG.[142] Because of its superior Young's modulus and comparable hydrophobicity to PLA-COOH and PLGA 75/25-COOH (details are referred to the previous subsection "Reverse Proof of Complex Physicochemical Properties Interplays"), it is very plausible that the nonsphericity of PBLG nanoparticles may stay longer in an aqueous dispersion in physiological-related condition. The lower bulk T_g of PBLG does not appear to significantly induce the nonspherical shape instability.

Whereas the latter instance is exhibited by the crystalline lipids (e.g., triglycerides) in spherical solid lipid nanoparticles, which is stored in aqueous medium at room temperature.[163,164] Triglyceride has high degree of hydrophobicity (Figure 5e; represented as cocoa butter[58]), bulk Young's modulus ≈0.25–0.47 × 10^{-6} GPa,[165] and average T_m 31–34 °C[58] (actual T_m ranging 11-73 °C[116] due to the variation of trilaurin-tristearin as well as α- & β-polymorph). Considering these unsupportive properties for nonsphericity, it is really astonishing to know that triglyceride nanoparticles can arrange themselves into nonspherical nanoparticles during storage. It is likely because of the necessity to have as high as possible cohesiveness[146] and density of crystal lattice.[164] In fact, the internal nonspherical (e.g., rod) crystal habit in nanoparticles can accommodate these needs through the formation of certain internal structure, i.e., stable β-polymorph.[115,160,161]

However, because both nonspherical PBLG and triglyceride nanoparticles already have the highest thermodynamic stability and molecular compactness, they may impart very poor drug loading[164,166] and final preparation quality. These situations are absolutely unexpected for drug delivery. In the future, we believe that the excellent compromise of shape factor and other manufacturing aspects will become the key issues to be handled. Additionally, in accordance with the findings described

in this section and our entire results, we can conclude that the internal structure is principally the most influential aspect in determining the longevity of nanoparticle shape, then followed by surface chemistry (bulk-nanoparticle hydrophobicity; which can be further divided into: residual stabilizers, core–shell structure, and not to mention surface roughness), and next by T_g-Young's modulus (nanoparticle integrity) in the equal position.

3.3. Effect of Porosity of Particles

In many cases, porosity may correlate inversely with the Young's modulus. It can be reflected from the relation of porosity (Figure 1g) and Young's modulus (Figure 1f) on nanoparticles prepared without any stabilizer or surfactant. The two most porous nanoparticles in this group (i.e., PLGA 50/50-COOH and gelatin) have the smallest Young's modulus. This trend was same as reported elsewhere.[167] These two factors appeared to be the additional inducers (beside surface roughness) to explain the poor nonspherical stability of PLGA 50/50-COOH nanoparticles by nanoprecipitation.

The degree of SSA gain depends on the type and concentration of used stabilizer[168,169] as well as sort of organic solvent.[170] These parameters are the renowned defining factors impacting the mechanical and hydrophobic properties of nanoparticles, thus also potentially affect the nonspherical nanoparticle shape stability. In addition, it has been studied the effect of diverse nanoparticle porosities[56,171] to the physiological-related events, such as protein adsorption.

The behavior of water absorbed into nanoparticles (displayed by the residual moisture) may be associated with various reasons, e.g., the effect of capillary condensation, the confinement of water by polymer structure, the formation of clusters, or the strong interactions between the highly bipolar water molecules and the polymer polar groups.[40]

3.4. Effect of Hydrophobicity of Materials and Particles

The presence of hardly removed residual stabilizers (usually surfactants) appears to be uncompromised for keeping the nonsphericity of nanoparticles in aqueous and/or physiological medium, chiefly when the bulk material is hydrophobic. Our hypothesis is totally based on our current experimental data and well supported by other references as discussed below.

3.4.1. Aliphatic Polyesters and Residual Stabilizers Thereof

For the first example PVA (Mowiol 4-88), an amphiphilic stabilizer (which was added in the emulsion solvent extraction process for aliphatic polyester nanoparticles preparation) and commonly used in the colloidal suspension, plays an important role in maintaining significantly longer the nonspherical nanoparticle shape stability. It is very interesting because the resulted nonspherical nanoparticles had been thoroughly washed. This may be explained that PVA molecules are supposed to stay at the nanoparticle–water interface after their

work to decrease the interfacial tension (i.e., nanoparticle surface energy per unit area) during the initial nanoparticle formation. It has also been reported that PVA may be adsorbed or tightly associated with the surface layer and thus cannot be completely removed from the surface of nanoparticles.[50,105,135] In general, PVA has been preferentially chosen as emulsifier in nanoparticles fabrication due to its excellent stabilizing ability to avoid particles aggregation during postpreparative steps (e.g., freeze-drying and purifying), high yield of dry particles powder, and ease to be redispersed in solution after lyophilization.[127] But, the interest of PVA use in biodegradable nanoparticle formation was rather low because of the reported health risk caused by PVA.[172] Nevertheless, recently PVA's safety profile is vindicated and acknowledged as "acceptable."[173] As a consequence, PVA is now already approved for several injection products by US Food and Drug Administration (FDA).[174]

In our results, residual PVA might arise dominantly from Mowiol 4-88 (stabilizer in emulsion solvent extraction method) instead of Mowiol 40-88 (matrix for film-stretching). This was confirmed by virtually no additional PVA adsorption onto nanoparticle surface after stretching and thorough washing of nonspherical aliphatic polyester nanoparticles fabricated by nanoprecipitation (Figure 5d), thus no improvement of nonspherical shape stability for aliphatic polyester nanoparticles fabricated by nanoprecipitation as well (Figure 1d). In contrary, the PVA content in aliphatic polyester nanoparticles was remarkably higher (Figure 5d). The disparity of PVA adsorption may be delineated by the interfacial activity variance of these PVAs,[121] beside the probable higher propulsion force inducing PVA entrapment during the nanoparticle formation. Mowiol 4-88 (stabilizer), the quite low molecular weight (31 kDa) PVA with the degree of hydrolysis 88%, has surface tension ≈45 mN m^{-1} at critical micelle concentration (CMC) 0.5% (our results were in accordance with the manufacturer), meaning quite high interfacial activity. This makes it as an exceptional stabilizer for dispersed system.[121] Hence, it was not surprising that Mowiol 4-88 is chosen one the most commonly used PVA in the production of biodegradable nanoparticles.[2,175] Whereas Mowiol 40-88, the large molecular weight (205 kDa) variant of PVA with degree of hydrolysis 88%, generates surface tension ≈54 mN m^{-1} at CMC 0.5%, which can be attributed to the relatively smaller interfacial activity. This fact may provide reliable reasons: a) why Mowiol 40-88 penetration and binding to the aliphatic polyester or compact nanoparticles are low and b) why it still can disrupt and strongly attach to the hydrophobic gelatin nanoparticles. In general, the lower molecular weight and degree of hydrolysis of PVA impart higher interfacial activity.[121]

According to our results, it is highly recommended to disclose the stabilizer details (e.g., for PVA, at least the information of molecular weight and degree of hydrolysis are vital to foretell the interfacial activity). Otherwise, the residue thereof becomes more uncertain and uncontrollable. However, some publications tend to disguise the information partly[176,177] or totally,[178,179] likely due to the confidentiality issue.

Besides, the unclear details of nanoparticle materials emanate as well. For example, some papers did not state clearly the molecular weight (/intrinsic viscosity)[177] and/or end group[180]

of used aliphatic polyesters; whereas these material properties are some of the determining factors for hydrophobicity. Our study and others[50] have shown clearly that the higher the hydrophobicity, the higher residual PVA, thus it may really modulate the nonspherical nanoparticle shape stability.

Furthermore, it is also really important to state the exact details of nanoparticle washing step (e.g., for centrifugation, it includes: the condition (speed and temperature), exact centrifugation cycle number and dilution factor; as well as dispersing energy[181]) during their synthesis. It was reported that the residual stabilizers on the nanoparticles are very determined by the degree of washing.[107,182] There are, however, practically no publications stating obviously all details of washing steps, and here, we propose to cope with it. The unknown washing step details make residual stabilizer issue more challenging and unpredictable. Of course, this issue is extremely critical for nonspherical shape stability.

Based on above findings, we can infer that the detail descriptions of employed materials (i.e., stabilizers and polymers) and washing steps in nanoparticle formation are very essential and should be declared as explicit as possible.

3.4.2. PS-COOH and Residual Stabilizers Thereof

The second residual stabilizers are based on the results of PS-COOH nanoparticles. It is very reasonable that no significant shape alteration is reported for elongated PS nanoparticles[4,6,13,19,83] because the nanoparticles may contain considerable amount of residual surfactants.[43,183] Although some commercial nanoparticle products contain surfactants as stabilizers, sometimes the manufacturers refuse to disclose the chemical nature of the surfactant used.[184] Only few studies (including ours) successfully characterized the concealed surfactant by manufacturer, such as sulfate salt surfactant in PS nanoparticles.[43]

3.4.3. Silica (SiO$_2$) and Residual Stabilizers Thereof

Beside our results, it was also reported that considerable amount of surfactant (i.e., CTAB) was left on nonspherical SiO$_2$ nanoparticles compared to spherical ones.[53] Li et al.[55] observed as well that besides good resistance of nonsphericity, the residual surfactants on nonspherical SiO$_2$ nanoparticles might help nanoparticles to be less degraded in simulated body fluids, such as gastric, intestinal, and blood. Also, they observed that the larger aspect ratio the nanoparticles, the more stable the nanoparticles against degradation in simulated body fluids. Based on this result, the larger aspect ratio might be correlated to the higher residual surfactants, protecting from harsh pressure effect of water.

3.4.4. Related Issue of Residual Stabilizers

By applying film-stretching method, it is very reasonable that the configuration of residual (semicrystalline polymeric;, e.g., PVA [in our study], PEG [3000–20 000],[185] poloxamer,[186] etc.)

ADVANCED
SCIENCE NEWS
www.advancedsciencenews.com

ADVANCED
HEALTHCARE
MATERIALS
www.advhealthmat.de

stabilizers alters significantly, such as from "mushroom" to "brush" (Figure 1a). The configuration alteration is attributed to our results that all stretched nanoparticles roughened after stretching [Figures 1f, 5a,b]). The "brush" conformation is renowned for much lower hydrophobicity because of thicker polymeric layer.[187] It was reported that the stretching of the polymer chains perpendicular to the surface leads to several new physical phenomena, including higher hydrophilicity.[187] Nevertheless, it is also important to note that film-stretching method can yield lower total system density as a result of surface area growth, leading to lesser protection by stabilizer at the interface (Figure 1d). It is prominent that lower density at the interface may cause the "mushroom" conformation.[188] Therefore, we suggest that the dynamic transition from "brush" to "mushroom" conformation does exist in the nonspherical particles manufactured by stretching method. This transition is in the contrary as usually reported in the spherical nanoparticles (from "mushroom" to "brush").[189]

In general, it appears convincingly that the density factor is slightly more dominant than conformation aspect. The most recent evidence is that the higher degree of stretching (including biaxial than uniaxial stretching; see Figure 1d and Supplemental Calculation, Supporting Information), the more likely the increase of hydrophobicity, thus resulting the lower C3 complement adsorption.[4] It is well known that C3 complement has greater adsorption propensity to more hydrophilic surface.[111,190] C3 behavior is quite anomalous, whereas the majority of opsonins exhibits faster and higher adsorption to more hydrophobic objects.[191]

Residual stabilizer issue is frequently underestimated[192] and misconstrued.[193] In the former case, it has been reported that the researchers claimed to use the "uncoated" nanoparticles. However, they actually used 1% PVA (without any further specification) on their formula.[192] Therefore, the definition of "uncoated" nanoparticles should be standardized to minimize the misleading and misinterpretation of experimental results caused by the unintentional nescience. In the latter case, nevertheless the study objective is good (i.e., to see the synergistic between nanoparticle surface properties and in vitro related outcome [cytotoxicity enhancement of doxorubicin]), it is likely that the cancer cell culture study using aliphatic polyester nanoparticles produced by emulsion solvent extraction elicit bias results because of the unwary washing step (very likely just one time) and the usage of great amount of certain stabilizers above CMC (i.e., Cremophor EL, Solutol HS 15, and Tween 80; in-between one-to-three orders of magnitude). Our speculation is based on another report[194] and our stabilizer physicochemical properties analysis (**Table 3**; further discussed in the next section); where these two stabilizers are very plausible to not present at the interface, thus detach easily from hydrophobic aliphatic polyester nanoparticles.

Furthermore, it is also important to note that toxicity can arise from residual stabilizers on a nanoparticle synthesis. However, on many occasions complete depletion of these residues is often difficult and sometimes impossible. The degree of stabilizer removal depends strongly to its affinity into nanoparticle matrix. For example, CTAB, which has relatively intermediate-high surface polarity (≈ 0.53) compared to other stabilizers (Figure 5e), is difficult to remove from hydrophilic matrix, such as silica[195] (Figure S4, Supporting Information). It was reported that thorough CTAB elimination may lead to aggregation of the nanoparticles.[196] The strongly positive charge of CTAB adsorbed onto the surface of nanoparticles can trigger cytotoxicity and rapid opsonization, succeeded by MPS clearance.[197] As a consequence, many novel manufacturing methods involving materials extracted from natural sources as a novel stabilizers (e.g., HSA, bovine serum albumin (BSA), etc.) have been studied to produce various core nanoparticle materials, such as aliphatic polyester[134] and gold.[198]

Additionally, the affinity of stabilizer onto nanoparticle surface may also be influenced by pH in the particular ionic stabilizers (Table 3; log$D$), such as sodium cholate, sodium deoxycholate, and Solutol HS 15. Nevertheless, some ionic stabilizers (e.g., sulfate ester group: SDS or docusate sodium) are less prone to the log$D$ alteration, thus enable them to better protect the nonspherical nanoparticles throughout various physiological pH (e.g., nonspherical nanoparticles which are intended for oral administration route[139]).

3.4.5. Investigation, Elaboration, and Outlook of Residual Stabilizers

To extensively and systematically appraise the root causes of different residual stabilizer extent and affinity in nanoparticle system, we suggest to investigate the primary and secondary interfacial activity parameters of several commonly used stabilizers and materials for particle formation. The former include SFE, interfacial tension, and WCA (Figure 5e). While, the latter consist of a) work of adhesion (also known as adhesion energy) between particle and stabilizer material in certain medium, i.e., water (WoA$_3$), b) interfacial tension of core particle and stabilizer material (IFT$_{1,2}$), and c) the difference of WoA$_3$ and IFT$_{1,2}$ (Figure S4, Supporting Information).

In the first priority, we propose to observe the difference of WoA$_3$ and IFT$_{1,2}$ to better represent the overall affinity between stabilizer and particle materials, which also complements the WoA$_3$ and IFT$_{1,2}$ concepts. It was already known that WoA$_3$ only demonstrates the short-term affinity, while IFT$_{1,2}$ describes the tension left in the formed bond (i.e., the bond's potential to break), characterizing long-term affinity.[199] From the deduction of our results and others,[53,124,127,129,133,135,136,168,194] the nonwashability of PVA, sulfate esters, CTAB, and Triton X-100 from various nanoparticles may strongly correlate to their primary and secondary interfacial activity parameters (Figure 5e and Figure S4, Supporting Information). Interfacial-activity-based algorithms to determine the stabilizer nonwashability and suitability for particle formation are suggested (Figure S4c, Supporting Information).

To scrutinize the physicochemical properties that could be linked to the behavior and pattern of residual stabilizers on nanoparticle, we propose to investigate further some examples of small molecule stabilizers discussed previously here, by virtue of comparing their other, yet related experimental and computational physicochemical parameters (Table 3). Alongside the normal reported basic physicochemical parameters for (active) substances, we consider to introduce a

Table 3. Physicochemical properties of small molecule stabilizers or surfactants frequently utilized in biomedicine–pharmaceutical area.

Code[e]	Material	Ionic type [+/−/0]	MW [Da]	Liquefaction Temperatures[58] [°C]	CMC (critical micelle concentration)[58] [%]	Material–water interfacial tension at CMC[58] [mN m−1]	HLB Experimental[58]	HLB Calculation[a]	LogP[b]	LogD[b] (at pH 7.4)	6.8	5.0	1.2	Intrinsic solubility[c]	PSA (polar surface area)[d] [Å²]
a	TPGS	0	1513	$T_g \approx -7.5$,[246]; $T_m \approx 41$[247]	0.02	45	≈13.2	9.15	8.81	8.81	8.81	8.81	8.81	−0.91 logS	257.43
b	CTAB	+	364.5	T_g N/A[j]; T_m 232–247	0.033–0.036	≈33[248]	N/A	7.38	2.69	2.69	2.69	2.69	2.69	−6.98 logS	0
c	SDS	−	288.4	T_g N/A[j]; T_m 204–207	0.24	25.2	40	40.00	2.04	2.04	2.04	2.04	2.22	−5.24 logS	74.81
d	Docusate sodium	−	444.6	T_g N/A[j]; T_m 153–157	0.11 / ≈0.02–0.03[249]	28.7	32[168]	24.35	2.86	2.86	2.86	2.86	3.42	−6.33 logS	118.18
e	Triton X-100	0	647	T_g N/A[j]; T_m 6	≈0.02[250]	≈30[251]	N/A	3.58	4.15	4.15	4.15	4.15	4.15	−4.59 logS	29.46
f	Na-cholate	−	430.5	T_g N/A[j]; T_m 236[252]	0.63[250,253]	≈40[248]	18[254]	22.87	2.48	−0.35	0.18	1.84	2.47	−3.70 logS	100.82
g	Na-deoxycholate	−	414.6	T_g N/A[j]; T_m 238–361[252]	0.41[253]	≈42[248]	16[254]	20.97	3.79	1.11	1.66	3.28	3.78	−5.02 logS	80.59
h	Polysorbate 20	0	1227	T_g N/A[j]	≈0.0013[255]	≈33[255]	16.7	10.60	2.39	2.39	2.39	2.39	2.39	−4.45 logS	133.14
i	Polysorbate 80	0	1310	T_g N/A[j]	≈0.0013[256]	42.5	15.0	8.23	5.05	5.05	5.05	5.05	5.05	−7.10 logS	133.14
j	PEG	0	350	T_g N/A[j]	0.001–0.1 monomer units [mol L⁻¹][257]	≈44	N/A[j]	14.77	−1.54	−1.54	−1.54	−1.54	−1.54	0.72 logS	105.07
			400	T_g N/A[j]		≈44	N/A[j]	15.05	−1.58	−1.58	−1.58	−1.58	−1.58	0.78 logS	114.30
			4000	T_g −98 – ←−17,[185]		≈55[h] – ≈65[257]	N/A[j]	32.54	−5.39	−5.39	−5.39	−5.39	−5.39	UCN[i]	861.93
			5000	T_m 50 – 58		≈55[h] – ≈65[257]	N/A[j]	37.39	−6.47	−6.47	−6.47	−6.47	−6.47	UCN[i]	1074.22
			6000	T_g −98 – ←−17,[185]; T_m −17,[185]; T_m 55–63		≈55[h] – ≈65[257]	N/A[j]	42.22	−7.55	−7.55	−7.55	−7.55	−7.55	UCN[i]	1286.51
k	(m)PEG[f]	0	350	T_g −50,[258] T_m 0–20,[258]	N/A[j]	N/A[j]	N/A[j]	14.44	−0.89	−0.89	−0.89	−0.89	−0.89	0.54 logS	94.07
			4000	T_g N/A[j]	N/A[j]	N/A[j]	N/A[j]	31.93	−4.75	−4.75	−4.75	−4.75	−4.75	UCN[i]	850.93
			5000	T_g N/A[j]	N/A[j]	N/A[j]	N/A[j]	36.76	−5.83	−5.83	−5.83	−5.83	−5.83	UCN[i]	1063.22
			6000	T_g N/A[j]	N/A[j]	N/A[j]	N/A[j]	41.60	−6.91	−6.91	−6.91	−6.91	−6.91	UCN[i]	1275.51
l	Cremophor EL	0	2474	T_g N/A[j]; T_m 19–20	≈0.002	40.9	12–14	9.47	14.70	14.70	14.70	14.70	14.70	19.63 logS	462.64
m	Solutol HS 15	0	948	T_g N/A[j]; T_m ≈30	0.005–0.02	42.3[259]	14–16	12.85	0.34	0.31	0.88	2.40	2.73	0.21 logS	216.21

a–d)Calculated using the Calculator Plugins in MarvinSketch software version 17.1.23.0 (2017), ChemAxon (http://www.chemaxon.com).[260] The used method was a)Chemaxon; b)Consensus method. All settings were set to default. Otherwise specified, the (parent) material molecular structures for calculation were obtained either from primarily ChemSpider (http://www.chemspider.com) or secondarily PubChem (https://pubchem.ncbi.nlm.nih.gov). e)Each molecular structure, used for imparting physicochemical properties by the computational method, is available in Figure S5 (Supporting Information). b)LogD is analogous with logP (partition coefficient), but it provides more specific partition coefficient at different pHs. Selected pH values represent various common physiological pHs, namely circulation system[261] and tissue or both so-called extracellular[262]_interstitia[263] (≈7.4), intestinal fluid (6.8),[264] endosomal[265]—endo-lysosoma[l266] or generally so-called intracellular (5.0; 4.0–6.5), and gastric fluid (1.2);[264] c)The smaller the value, or the more negative the log value, the lower the substance solubility in water; d)PSA values are identic at various pHs and calculated by inclusion of all atoms; f)PEG: (mono)methoxy poly(ethylene glycol); the common hydrophilic component for formation of block copolymer with aliphatic polyesters; g)The relation of trade: *generic name: Triton X-100: (4)octyl phenol (poly)ethoxylate; Cremophor EL: Polyoxyl 35 Castor Oil; Solutol HS 15/ Kolliphor HS 15: Polyoxyl 15 Hydroxystearate;* h)10% w/v substance in HPW; i)UCN: Unable to be calculated because of too complex molecular structure; j)N/A: Not Available.

ADVANCED
SCIENCE NEWS
www.advancedsciencenews.com

ADVANCED
HEALTHCARE
MATERIALS
www.advhealthmat.de

novel parameter, namely molecular polar surface area (PSA). PSA is the total area on molecule surface exerting merely polarized atoms (e.g., ultimately oxygen and nitrogen, also encompassing their bound hydrogens).[200] By this way, researchers can predict the partition degree of substances (in a diverse way as the conventional one, e.g., partition coefficient [$\log P$ and $\log D$]), thereby estimate the molecular hydrophobicity,[201] conformation evolution,[202] as well as behavior towards various cell membranes recently.[203,204] PSA calculation gives results, which are proportionally comparable with the accessible surface area (ASA)[205] representing area of a molecule that is accessible to solvent (i.e., water). Additionally, PSA is approximately up to two order magnitudes faster than ASA analysis.[200] The greater the PSA value (for instance ≥ 140 Å^2[203]), the more hydrophilic the substance, thus the poorer imbalance between hydrophilic and hydrophobic (or lipophilic) part of the substance, leading to its lower interaction to the more amphiphilic matters (i.e., cell membrane). Therefore, it is not surprising that higher PSA displays poor membrane or cell permeation, e.g., through intestine[203,206] or blood–brain barrier (BBB).[206,207] In contrary, the lower PSA value (i.e., ≤ 60 Å^2) was reported to have better equilibrium between hydrophilic and hydrophobic, hence the interplay between the substance and amphiphilic substrates occurred stronger.[203]

Through this inspiration and the comparison of cumulative physicochemical properties of small molecule stabilizers (Table 3, Figure 5e and Figure S4, Supporting Information), it is getting clear that generally, nonwashable stabilizers should have a certain proportion of polar (hydrophilic) and disperse (hydrophobic or non-polar) (or so-called surface polarity, X_p) depending on the nature of particles, thus it can support their resistance on particles. These nonwashable characteristics (of small molecule stabilizers) are possessed by, for example sulfate esters, Triton X-100, and CTAB, demonstrating these characteristics: low surface tension (<40 mN m^{-1}) at CMC, high $\log P$ (>2), high and virtually constant $\log D$ at various pHs (each >2), low intrinsic solubility (<–4.0 $\log S$), and PSA < 120 Å^2. Interestingly, hydrophilic–lipophilic balance (HLB) parameter, which is initially and frequently used as emulsion stability descriptor,[208] shows very poor correlation toward the residual stabilizers on nanoparticle system, which can be classified as suspension. Hence, HLB may be rather inappropriate to portray the stabilizer affinity on solids dispersed in liquid medium.

In addition, both interfacial activity parameters (Figure 5e) and other related physicochemical properties (Table 3) may also be appropriate to elucidate the inability reason of several general stabilizers (e.g., polysorbate 80,[194] gelatin,[194] poly(vinylpyrrolidone) (PVP),[194] and PEG (4000)[209]) in assisting the formation of nanoparticles. It is strongly proven that these stabilizers were deviated widely from the suggested values (Figure 5e and Figure S4, Supporting Information and Table 3). Our databases may complement the old report of Albertsson,[210] still displaying no quantitative comparison between the macromolecular stabilizers. Nevertheless, his work is really influential to date and widely applied in pharmaceutical area[106,211] to give insight of material (macromolecule) and nanoparticle hydrophobicity. In accordance with

Albertsson's report, dextran and its derivatives are the most hydrophilic polymers, while PVA and PEG have quite similar hydrophilicity (with PVA shows higher hydrophilicity). It can explain why dextran is totally not sufficient as stabilizer for hydrophobic aliphatic polyester nanoparticles development,[194] but fails to enlighten, why the more hydrophilic PVA can be a great stabilizer than PEG (4000[209]) for (aliphatic polyester) nanoparticle synthesis. In fact, to be bond with the hydrophobic aliphatic polyesters, the relatively more hydrophobic PEG variants (i.e., commonly methoxyPEG [(m)PEG] 2000,[212] 3400,[213] till 5000[212,214]) should be covalently linked onto the aliphatic polyester backbone forming the block copolymer; where these block copolymers may form (micelle-like) nanoparticles in aqueous solution. Logically, if the Albertsson's sequence is assumed to be fully valid, the PEG may exhibit spontaneous and higher adsorption onto hydrophobic aliphatic polyesters. The combination of interfacial activity parameters (Figure 5e) and other related physicochemical properties of stabilizers (Table 3) may clarify such PEG issue, i.e., PEG has too weak interfacial activity (SFE or surface tension ≈ 55–65 mN m^{-1}), too high solubility in water (positive $\log S$) and high PSA ($> \approx 1000$ Å^2), thus shows practically no presence at the interface due to its higher affinity to water molecules. In conclusion, the physicochemical properties generated by the computational method appear to be promising to equip our interfacial activity knowledge in comprehending its relation to the residual stabilizers.

Meanwhile, in case of big molecule (termed as macromolecule afterwards) stabilizers, hitherto it is still rather hard to connect the residual macromolecule stabilizer on nanoparticle with their physicochemical properties due to the lack of appropriate physicochemical descriptor to be linked and great complexity-plausibility of interactions. Also, even by means of computational simulation, it requires a lot of computation effort, time, and cost just for the basic physicochemical properties (e.g., T_g, WCA, etc[215]). Therefore, to date the limited experimental approach (i.e., interfacial activity parameters; Figure 5e) is the only source to understand this phenomenon. Nevertheless, we believe that the progress of macromolecule experimental and computational research will provide tools to unveil the holy grail of residual macromolecule stabilizer on nanoparticles. Recently, the novel trend to use computer-assisted drug formulation design commenced.[216]

As an outlook, we envision that certain residual stabilizers can be vexed, both for manufacturing process and clinical translation of nonspherical nanoparticles. This is due to the fact that albeit implementation of clearly described and strictly standardized nanoparticle washing as shown in this report, in many cases we cannot neglect the existence of particular residual stabilizers. On the one hand, they can be an impressive companion for particle shape stability, yet modulate other nanoparticle physicochemical properties (e.g., Young's modulus, surface roughness, T_g, porosity, residual moisture, and hydrophobicity). On the other hand, they may also be a potential threat for further clinical application because almost all strongly retained stabilizers on nanoparticles are renowned for their toxicity. Careful selection of currently available stabilizers and innovative material development are demanded for the advancement of nonspherical nanoparticles. Besides, the clear divulgence of used

**ADVANCED
SCIENCE NEWS**

www.advancedsciencenews.com

**ADVANCED
HEALTHCARE
MATERIALS**

www.advhealthmat.de

stabilizer and washing process is very imperative. In the future, the nanoparticle research results should be more cautiously evaluated due to the inseparable influence of particle shape and surface chemistry.

3.5. Comparison to Nonspherical Silica (SiO$_2$) Nanoparticles and Other Systems

Learning from excellent shape stability of SiO$_2$ nanoparticles (still having residual stabilizers) in physiologically relevant condition, the further question may arise. How come if there are no residual stabilizers (or surfactants) at all during the manufacturing process? Could the nonspherical shape of nanoparticles dispersed in aqueous physiologically mimicking environment still persist? The answer is likely yes, but the Young's modulus and liquefaction temperature (either T_g or T_m) of the material should be exceptionally high. For example, very hydrophobic single-walled carbon nanotube (SWCNT), having T_m of 4177 °C[217] and Young modulus of 1800 GPa making it as one of the stiffest material measured experimentally[218]), can be produced spontaneously without the presence of stabilizer using arc-discharge evaporation.[219] This technique is the same as to produce other fullerenes, such as spherical C$_{60}$ (also, so-called Buckminsterfullerenes or buckyballs). Based on this, the member of fullerenes family may have similarity in terms of very great hydrophobicity. It has been reported that experimentally, spherical fullerenes are the most hydrophobic nanoparticles (regardless of their fabrication method) relative to gold and silver nanoparticles formulated with various stabilizers.[220] It seems that their results concerning sequence of nanoparticle hydrophobicity may have a good correlation to the bulk material hydrophobicity (Figure 5e; case: gold vs unwrapped SWCNT). Therefore, we believe that the interfacial activity database coupled by complete bulk-nanoparticle physicochemical properties may be an initial guidance (after internal structure status) to appraise the nonspherical particle shape stability in the dispersion medium. Since our interfacial activity database covers only the aqueous data, it is required more elaboration to provide similar database for nonspherical shape stability prediction in other dispersion medium (e.g., organic solvent, oil, etc.), which may be interesting for other research areas.[83,149]

Nevertheless, nothing is perfect in this world. Albeit the high plausibility of stable nonsphericity, fullerenes family inclines to flocculate in order to avoid their dispersion in solvents or viscous polymer melts[221] due to their very hydrophobic nature. Stabilizers with highly strong interfacial activity and low-intermediate surface polarity (about 44%, e.g., sulfate esters (specifically docusate sodium) and Triton X-100;[222] recall Figure 5e and Table 3) are generally required to disperse the fullerenes family in aqueous dispersion medium. It can be proven with our database (Figure 5e) and secondary interfacial activity parameter calculation, resulting the conclusion that both stabilizers are very likely nonwashable from SWCNT (e.g., Triton X-100 with WoA$_3$ 25.51, IFT$_{1.2}$ 7.72, and the difference of WoA$_3$-IFT$_{1.2}$ 17.79 mN m^{-1}). However, again the inextricability of particle shape and surface chemistry (as well as other physicochemical properties) is highly accentuated.

3.6. Lesson Learned from Nonspherical Particle Shape Stability

To make the inference of nonspherical particles shape stability, we should take into account all manufacturing aspects (including bulk and nanoparticle form) as well as their consequences to physicochemical properties. Otherwise, the fallacy is obtained. For example, if merely the hydrophobicity, molecular weight/viscosity, and T_g properties in the bulk form are taken into account, it will be reasonable to put PLGA 50/50-COOH nanoparticles as the long-lasting nonspherical nanoparticles between the aliphatic polyesters produced by nanoprecipitation. In fact, it had the poorest shape stability between the aliphatic polyesters prepared by nanoprecipitation. Relatively neglected properties (such as nanoparticle integrity, nanoparticle Young's modulus, nanoparticle surface roughness, nanoparticle wet T_g, nanoparticle porosity, and residual stabilizers in nanoparticles) prove clearly that they should also be carefully and simultaneously assessed. Another instance is O-CMCHS. Despite its great bulk hydrophilicity (Figure 5e) and T_g (140–150 °C),[81] the nonsphericity of O-CMCHS nanoparticles is the worst among other materials studied here. Lack of nanoparticle integrity is responsible for this reason.

In contrary, we cannot conclude the nonspherical shape stability based on only the (partial) nanoparticle properties. For instance, gelatin nanoparticles were the smoothest surface (R_{rms} = 3.2 nm) nanoparticles, which usually may lead to the lesser hydrophobicity degree.[37] However, nonspherical gelatin nanoparticles were ones of the least stable nanoparticles in terms of nonsphericity. This could not be separated from the poor nanoparticle integrity (demonstrated by swelling), relatively high porosity (1.57 m^2 g^{-1}), soft (nanoparticle Young's modulus of 0.7 GPa), and great hydrophobicity (both in bulk and nanoparticle forms; Figure 5d,e). Further example, SiO$_2$ nanoparticles have the highest porosity (generally ranging from tens to hundreds m^2 g^{-1}), that may be interpreted one of the risk of nonspherical shape instability. Nonetheless, because of very low hydrophobicity and great mechanical properties (high Young's modulus 73 GPa, acceptable surface roughness ≈2.5–10 nm, and T_m 1600 °C), it turns out that SiO$_2$ nanoparticles are ones of the most stable nanoparticles in terms of nonsphericity.

To sum up, in relation to the nonspherical particle shape stability, negative factors (high hydrophobicity, surface roughness, and porosity) of nanoparticles are counterbalanced by positive factors (existence of nonspherical structure, high stiffness, and liquefaction temperature). According to our experimental results and some available reports, the detail considerations of manufacturing aspects toward nonspherical shape stability and their potential biological relations are summarized in **Table 4**.

4. Conclusions

Particle shape is one of the most critical parameters in drug delivery. This momentousness should be verified further and heedfully for reliable in vitro and in vivo experiments. Our report strongly suggests that shape alteration tendencies of nonspherical particles (having no specific internal structure) to spherical particles may occur in favor of thermodynamic (due to trigger of material–water interfacial tension), and the

Table 4. Contrast and deliberation of manufacturing aspects toward (nonspherical) particle's physicochemical properties and their potential biological relations.

Advantages	Manufacturing aspects	Disadvantages

• ↑ Aspect ratio → ↓ probability for phagocytosis by macrophages[8,19] → ↑ circulation time[4]
• ↑ Surface area → ↑ "loading" of active pharmaceutical ingredients (APIs) (in case of APIs should be tethered onto surface[9,22,64,267])
• ↑ Polymer orientation and crystallinity* (*in case of semicrystalline ones) → ↑ rigidity and liquefaction temperatures (T_g and T_m) → ↑ nonsphericity stability
• ↑ Variance of particle's radius of curvature ($R_c(t)$) → ↑ choices for other unique related phenomenas (e.g., substance adsorption-stability, liquefaction temperatures [T_g and T_m], etc.)
• Bestow relatively same volume as the starting spherical* particles for better in vitro and in vivo study comparison (*as long as the integrity of particles is sufficient)
	Stretching (e.g., using film-stretching method)	• ↑ Surface area → ↑ possibility of APIs burst release
		• ↓ Density and amount* of stabilizer (*in certain case, e.g., P407 extracted by PVA[106])
		• ↑ Surface roughness
		• As above consequences: generally ↑ contact area of pressure and hydrophobicity → ↓ non-sphericity stability
		• ↑ Variance of particle's ($R_c(t)$) → ↑ presence, abundance & degree of highly curved surface areas → ↓ non-sphericity stability; in fact, highly curved areas / smaller ($R_c(t)$)s are already proven in vitro[268] and in vivo[118] to generally impact the following properties of adsorbed (blood) proteins:
		  ○ ↓ Total amount of adsorbed proteins
		  ○ Modulate cumulative adsorbed proteins' surface hydrophobicity (Φ_f) depending on particles' surface hydrophobicity:[269]
		    ■ ↓ ($R_c(t)$) on ↓ hydrophobic particles → ↑Φ_f[268]
		    ■ ↓ ($R_c(t)$) on ↑ hydrophobic particles → ↓Φ_f[118] → however, evidently the ↓Φ_f and quite ↓ total amount of adsorbed proteins can not avoid the strong confinement effect on ↓ liquefaction temperatures (T_g and T_m) that are caused by too ↓$R_c(t)$ → drastically ↓ nonsphericity stability[118]
		  ○ ↓ Cumulative negative charge of adsorbed proteins, leading to the ↓ zeta potential of particles

• ↑ Dissolution rate-solubility of APIs and permeability	(Nano-)size	• ↑ Polymer degradation • ↓ Surface-free energy and ↑ interfacial tension (~↑ hydrophobicity[211]) → ↑ pressure / force against particles → ↓ nonsphericity stability
	↑ surface area	
• ↑ Dissolution rate solubility and loading of APIs	Porosity	• ↑ Polymer degradation • ↑ Inclination of residual moisture → ↓ nonsphericity stability
• ↑ Permeability and cellular uptake	Hydrophobicity	• ↓ Nonsphericity stability • ↑ Total amount of adsorbed (blood) proteins & ↑ opsonization (especially for ↑Φ_f [blood] proteins[268,269])
• ↑ Viscosity, T_g, and rigidity → ↑ Non-sphericity stability* (*in case of non-washable stabilizer involvement during particle fabrication; e.g., emulsion solvent extraction)[26] • ↑ Degradation time	("High") molecular weight and viscosity of polymer	• ↑ Particles size & size distribution, porosity* (*in case of nonwashable stabilizer involvement) and surface area • ↓ Yield of fabricated nanoparticles (in case of nanoprecipitation) • ↓ elasticity and hydrophilicity • ↑ Interfacial tension
• ↓ Hydrophobicity (charged condition; pH is far from pKa) → ↑ nonsphericity stability	Functional group modification of polymer (viz. carboxyl-ended)	• ↑ Hydrolysis → ↓ degradation time (i.e., aliphatic polyesters) • ↓ Permeability → ↓ cellular uptake (by healthy cells) • ↑ Hydrophobicity (less-charged condition; pH is closer to pKa);[26] example: due to relatively more acidic intracellular compartment (Table 3) of healthy cells or extracellular compartment of cancer cells,[270] -COOH (pKa 3.85) is ↑ protonated → ↓ nonsphericity stability[26]
• ↓ Hydrophobicity by ↓ interfacial tension → ↓ adsorbability of (blood) proteins • ↑ Mechanical properties (in some variants, e.g., PVA enhancing Young's modulus & T_g) • ↑ Nonsphericity stability (by ↑ residual stabilizers; i.e., particular PVA, which may have biological disadvantages (as described on the right))	Stabilizers (e.g., PVA, poloxamer, TPGS, SDS, PEGylation, etc.)	(If too much and highly attached residual stabilizers onto particles) • ↑ Specific surface area (SSA; e.g., relatively more substantial SSA ↑ by PEG)[269,271] &/ ↓ liquefaction temperature (e.g., T_g by PEG[272] Triton X-100,[124] Poloxamers,[273] etc.) → ↑ burst release[124,269,271] &/ ↓ nonsphericity stability • ↓ Hydrophobicity → ↓ permeability & cellular uptake • ↑ Formation of specific antibodies (e.g., PEG)[274] → ↑ clearance of drug vehicles[275]

Table 4. Continued.

Advantages	Manufacturing aspects	Disadvantages
• Common & safe administration media for drug delivery system • ↑ Nonsphericity stability by formation of more stable polymorph[163,276]	Water (including humidity)	• ↓ Liquefaction temperatures (T_g[40] and T_m[277]) → ↓ nonsphericity stability by considerable interfacial tension discrepancy, specifically at less-charged condition (i.e., pH is closer to pKa [if any] of such particle material[26] in case of shape-memory polymeric particles) & ↓ particle's ($R_c(t)$) (including also metallic particles[117–119]) (Note: In agreement with compendia from several authorities,[278–280] the pH of highly purified water (HPW) should not necessarily be 7.0, but it can be between 5.0 and 7.0, as the used HPW here, i.e., pH 5.5-5.8 (~endosomal pH[265]) and elsewhere.[150] Thus, water aspect should be assessed carefully and on a case-by-case basis).
• ↓ Residual stabilizers until minimum depending on the nature of stabilizers (reportedly, purification efficiency of certain centrifugation ~Cross-flow filtration [CFF][127] aka tangential-flow filtration [TFF][281] aka ultrafiltration[282] ≥ gel permation chromatography [GPC][105] aka gel filtration chromatography [GFC] aka size-exclusion chromatography [SEC], especially for easily washable stabilizers, e.g., poloxamer groups[105]) → ↓ toxicity, but this may also bring disadvantages (as described on the right)	Purification	(if too "clean", particularly for easily washable stabilizers) • ↓ Nonsphericity stability & ↑ particle aggregation[196] chiefly in case of hydrophobic, porous and/or amorphous (no specific internal structure in) particles
(Only by particular compendial methods[278,280,283] [e.g., sterile filtration using membranes ≤ 0.22 µm or presterilization+aseptic processing] which still virtually maintain non-sphericity stability) • ↑ Sterility	Sterilization	(For sterile filtration) • Practically impossible to be applied to spherical particle Ø > 0.22 µm or nonspherical particle owing minor axes > 0.22 µm • May ↓ particle yield depending on the properties of particles (e.g., size, hydrophobicity, charge, etc.) (Many cases of compendial sterilization methods[278–280,283,284] e.g., a) steam [≥ 121 °C for 15 min], b) dry-heat sterilization [≥ 160 °C for ≥2 h], c) ionizing radiations [normally 25 kGy or 2.5 Mrad], either beta- or gamma-irradiation, and d) gas [e.g., ethylene oxide with residual limit ≤1 ppm[285]]) • Generally ↑ surface roughness[31] and residual moisture aka water content[286] • ↓ Young's modulus (in case of amorphous materials)[287] • Frequently ↓ molecular weights of polymers (especially for blank particles) → ↓ liquefaction temperatures (T_g and T_m[288]) & ↓ SSA → ↑ aggregation & ↑ possibility of APIs burst release[289,290] • As above consequences: ↓ Nonsphericity stability Nevertheless, sterilization aspect should still be assessed carefully and on a case-by-case basis
• ↑ Stability (e.g., cryoprotectants; if lyophilization is needed)	Other additional substances (e.g., APIs, excipients, etc.)	• ↓ Nonspherical stability (i.e., counter-ion,[26] substances causing preparation's pH ~pKa of [e.g., polymeric] vehicles,[26] loaded[158,291]/adsorbed hydrophobic substances[26] including proteins,[291] substances ↓ liquefaction temperatures of whole particles, such as gentamicin → also ↑ burst release,[290] [if applicable] residual oil during particle fabrication, etc.)
• ↑ Nonsphericity stability (e.g., PBLG[142])	(Stable, ordered and nonspherical) Internal structure/crystal system/crystallographic form	• ↓ Drug loading (e.g., stable β-polymorph of crystalline lipids, such as triglycerides[115,160,161] • ↑ Toxicity

rate at which this change occurred do not only depend on the bulk material properties and storage temperature, but also importantly on the physicochemical properties of the resulted nanoparticles. Besides, this rate of shape transformation can be simply tuned with the presence and extent of residual stabilizers. The evidence is displayed by decrease of aspect ratio (AR) and hydrodynamic size as well as PDI. In case of biodegradable polymeric nanoparticles, aliphatic polyester nanoparticles prepared by emulsion solvent extraction using certain PVA was remarkably superior in terms of nonspherical nanoparticle shape stability compared to nanoparticles fabricated by other stabilizers, purely nanoprecipitation method, different materials, and manufacturing techniques. It appears that the residual stabilizers can be a great companion for nanoparticles in maintaining their nonsphericity, if they are considered as a nontoxic, biodegradable, and biocompatible material.

Supporting Information

Acknowledgements

Conflict of Interest

The authors declare no conflict of interest.

Keywords

[1] a) G. Birrenbach, P. P. Speiser, *J. Pharm. Sci.* **1976**, *65*, 1763; b) V. Lenaerts, P. Couvreur, D. Christiaens-Leyh, E. Joiris, M. Roland, B. Rollman, P. Speiser, *Biomaterials* **1984**, *5*, 65; c) H. Fessi, J. P. Devissaguet, F. Puisieux, C. Thies, *French Patent* **1986**, *2*, 988; d) R. H. Müller, C. Lherm, J. Herbert, P. Couvreur, *Biomaterials* **1990**, *11*, 590; e) M. Klinger-Strobel, J. Ernst, C. Lautenschläger, M. W. Pletz, D. Fischer, O. Makarewicz, *Int. J. Nanomed.* **2016**, *11*, 575; f) A. C. Anselmo, S. Mitragotri, *Bioeng. Transl. Med.* **2016**, *1*, 10.

[2] D. Klose, F. Siepmann, K. Elkharraz, J. Siepmann, *Int. J. Pharm.* **2008**, *354*, 95.

[3] S. M. Moghimi, A. C. Hunter, J. C. Murray, *Pharmacol. Rev.* **2001**, *53*, 283.

[4] P. P. Wibroe, A. C. Anselmo, P. H. Nilsson, A. Sarode, V. Gupta, R. Urbanics, J. Szebeni, A. C. Hunter, S. Mitragotri, T. E. Mollnes, S. M. Moghimi, *Nat. Nanotechnol.* **2017**, *12*, 589.

[5] a) W. Lu, T. G. Park, *PDA J. Pharm. Sci. Technol.* **1995**, *49*, 13; b) W. L. Lee, Y. C. Seh, E. Widjaja, H. C. Chong, N. S. Tan, S. C. Joachim Loo, *J. Pharm. Sci.* **2012**, *101*, 2787.

[6] R. Mathaes, G. Winter, T. J. Siahaan, A. Besheer, J. Engert, *Eur. J. Pharm. Biopharm.* **2015**, *94*, 542.

[7] C. A. Fromen, T. B. Rahhal, G. R. Robbins, M. P. Kai, T. W. Shen, J. C. Luft, J. M. DeSimone, *Nanomedicine* **2016**, *12*, 677.

[8] R. Mathaes, G. Winter, A. Besheer, J. Engert, *Int. J. Pharm.* **2014**, *465*, 159.

[9] R. A. Meyer, J. C. Sunshine, K. Perica, A. K. Kosmides, K. Aje, J. P. Schneck, J. J. Green, *Small* **2015**, *11*, 1519.

[10] R. Agarwal, V. Singh, P. Jurney, L. Shi, S. V. Sreenivasan, K. Roy, *Proc. Natl. Acad. Sci. USA* **2013**, *110*, 17247.

[11] C. C. Ho, A. Keller, J. A. Odell, R. H. Ottewill, *Colloid Polym. Sci.* **1993**, *271*, 469.

[12] J. A. Champion, Y. K. Katare, S. Mitragotri, *J. Controlled Release* **2007**, *121*, 3.

[13] B. Felder, *Helv. Chim. Acta* **1966**, *49*, 440.

[14] L. C. Glangchai, M. Caldorera-Moore, L. Shi, K. Roy, *J. Controlled Release* **2008**, *125*, 263.

[15] R. Agarwal, V. Singh, P. Jurney, L. Shi, S. V. Sreenivasan, K. Roy, *ACS Nano* **2012**, *6*, 2524.

[16] V. Singh, R. Agarwal, P. Jurney, K. Marshall, K. Roy, L. Shi, S. V. Sreenivasan, *J. Micro. Nanomanuf.* **2015**, *3*, 011002.

[17] a) J. P. Rolland, B. W. Maynor, L. E. Euliss, A. E. Exner, G. M. Denison, J. M. DeSimone, *J. Am. Chem. Soc.* **2005**, *127*, 10096; b) E. M. Enlow, J. C. Luft, M. E. Napier, J. M. DeSimone, *Nano Lett.* **2011**, *11*, 808; c) S. W. Morton, K. P. Herlihy, K. E. Shopsowitz, Z. J. Deng, K. S. Chu, C. J. Bowerman, J. M. DeSimone, P. T. Hammond, *Adv. Mater.* **2013**, *25*, 4707; d) J. M. DeSimone, *J. Controlled Release* **2016**, *240*, 541.

[18] a) S. Xu, Z. Nie, M. Seo, P. Lewis, E. Kumacheva, H. A. Stone, P. Garstecki, D. B. Weibel, I. Gitlin, G. M. Whitesides, *Angew. Chem., Int. Ed.* **2005**, *44*, 724; b) N. Hakimi, S. S. H. Tsai, C.-H. Cheng, D. K. Hwang, *Adv. Mater.* **2014**, *26*, 1393; c) K. S. Paulsen, D. Di Carlo, A. J. Chung, *Nat. Commun.* **2015**, *6*, 6976; d) C. Hamon, M. Henriksen-Lacey, A. La Porta, M. Rosique, J. Langer, L. Scarabelli, A. B. S. Montes, G. González-Rubio, M. M. de Pancorbo, L. M. Liz-Marzán, L. Basabe-Desmonts, *Adv. Funct. Mater.* **2016**, *26*, 8053.

[19] J. A. Champion, S. Mitragotri, *Proc. Natl. Acad. Sci. USA* **2006**, *103*, 4930.

[20] a) J. A. Champion, S. Mitragotri, *Pharm. Res.* **2009**, *26*, 244; b) Arnida, M. M. Janát-Amsbury, A. Ray, C. M. Peterson, H. Ghandehari, *Eur. J. Pharm. Biopharm.* **2011**, *77*, 417.

[21] G. Sharma, D. T. Valenta, Y. Altman, S. Harvey, H. Xie, S. Mitragotri, J. W. Smith, *J. Controlled Release* **2010**, *147*, 408.

[22] J. C. Sunshine, K. Perica, J. P. Schneck, J. J. Green, *Biomaterials* **2014**, *35*, 269.

[23] J. E. Mark, *Polymer Data Handbook*, Oxford University Press, Oxford **1999**.

[24] B. K. Lee, Y. Yun, K. Park, *Adv. Drug Delivery Rev.* **2016**, *107*, 176.

[25] H. Fessi, F. Puisieux, J. P. Devissaguet, N. Ammoury, S. Benita, *Int. J. Pharm.* **1989**, *55*, R1.

[26] J.-W. Yoo, S. Mitragotri, *Proc. Natl. Acad. Sci. USA* **2010**, *107*, 11205.

[27] A. Bootz, V. Vogel, D. Schubert, J. Kreuter, *Eur. J. Pharm. Biopharm.* **2004**, *57*, 369.

[28] a) A. C. Anselmo, B. Prabhakarpandian, K. Pant, S. Mitragotri, *Transl. Mater. Res.* **2017**, *4*, 014001; b) J. Hrkach, D. Von Hoff, M. M. Ali, E. Andrianova, J. Auer, T. Campbell, D. De Witt, M. Figa, M. Figueiredo, A. Horhota, S. Low, K. McDonnell, E. Peeke, B. Retnarajan, A. Sabnis, E. Schnipper, J. J. Song, Y. H. Song, J. Summa, D. Tompsett, G. Troiano, T. Van Geen Hoven, J. Wright, P. LoRusso, P. W. Kantoff, N. H. Bander, C. Sweeney, O. C. Farokhzad, R. Langer, S. Zale, *Sci. Transl. Med.* **2012**, *4*, 128ra39.

[29] Polysciences; Inc, Polybead Microspheres, Product Information, http://www.polysciences.com/skin/frontend/default/polysciences/pdf/Polybead_Microspheres.pdf, Warrington **2011**, 2 (accessed: July 2019).

[30] P. Zhang, L. Yang, Q. Li, S. Wu, S. Jia, Z. Li, Z. Zhang, L. Shi, *ACS Appl. Mater. Interfaces* **2017**, *9*, 7648.

[31] R. Dorati, M. Patrini, P. Perugini, F. Pavanetto, A. Stella, T. Modena, I. Genta, B. Conti, *J. Microencapsulation* **2006**, *23*, 123.

[32] S. Tan, R. L. Sherman, W. T. Ford, *Langmuir* **2004**, *20*, 7015.

[33] N. Doshi, A. S. Zahr, S. Bhaskar, J. Lahann, S. Mitragotri, *Proc. Natl. Acad. Sci. USA* **2009**, *106*, 21495.

[34] M. P. Neubauer, C. Blum, E. Agostini, J. Engert, T. Scheibel, A. Fery, *Biomater. Sci.* **2013**, *1*, 1160.

[35] X. Han, S. Chen, X. Hu, *Desalination* **2009**, *240*, 21.

[36] R. Dingreville, J. Qu, C. Mohammed, *J. Mech. Phys. Solids* **2005**, *53*, 1827.

[37] P.-C. Lin, S. Yang, *Soft Matter* **2009**, *5*, 1011.

[38] a) M. W. Lee, S. S. Latthe, A. L. Yarin, S. S. Yoon, *Langmuir* **2013**, *29*, 7758; b) A. Opdahl, G. A. Somorjai, *J. Polym. Sci., Part B: Polym. Phys.* **2001**, *39*, 2263.

[39] R. Steendam, M. J. van Steenbergen, W. E. Hennink, H. W. Frijlink, C. F. Lerk, *J. Controlled Release* **2001**, *70*, 71.

[40] P. Blasi, S. S. D'Souza, F. Selmin, P. P. DeLuca, *J. Controlled Release* **2005**, *108*, 1.

[41] C. Zhang, Y. Guo, R. D. Priestley, *Macromolecules* **2011**, *44*, 4001.

[42] U. Gaur, B. Wunderlich, *Macromolecules* **1980**, *13*, 1618.

[43] T. Sasaki, A. Shimizu, T. H. Mourey, C. T. Thurau, M. Ediger, *J. Chem. Phys.* **2003**, *119*, 8730.

[44] V. Le Brun, W. Friess, S. Bassarab, P. Garidel, *Pharm. Dev. Technol.* **2010**, *15*, 421.

[45] B. Semete, L. Booysen, Y. Lemmer, L. Kalombo, L. Katata, J. Verschoor, H. S. Swai, *Nanomedicine* **2010**, *6*, 662.

[46] T. R. Fadel, E. R. Steenblock, E. Stern, N. Li, X. Wang, G. L. Haller, L. D. Pfefferle, T. M. Fahmy, *Nano Lett.* **2008**, *8*, 2070.

[47] N. Sugita, K.-i. Kawabata, K. Sasaki, I. Sakata, S.-i. Umemura, *Bioconjugate Chem.* **2007**, *18*, 866.

[48] W. Alewelt, *Technische Thermoplaste. 4. Polyamide*, Hanser, Munich, Germany **1998**.

[49] D. P. Joshi, Y. L. Lan-Chun-Fung, J. G. Pritchard, *Anal. Chim. Acta* **1979**, *104*, 153.

[50] K. M. Shakesheff, C. Evora, I. Soriano, R. Langer, *J. Colloid Interface Sci.* **1997**, *185*, 538.

[51] a) R. Defay, A. Bellemans, I. Prigogine, *Surface Tension and Adsorption*, Longmans, London **1966**; b) R. J. Hunter, *Foundations of Colloid Science*, Oxford University Press, Oxford **2001**.

[52] a) Q. Cai, Z.-S. Luo, W.-Q. Pang, Y.-W. Fan, X.-H. Chen, F.-Z. Cui, *Chem. Mater.* **2001**, *13*, 258; b) J. G. Croissant, Y. Fatieiev, N. M. Khashab, *Adv. Mater.* **2017**, *29*, 1604634; c) F. Tang, L. Li, D. Chen, *Adv. Mater.* **2012**, *24*, 1504; d) N. Hao, L. Li, F. Tang, *Int. Mater. Rev.* **2017**, *62*, 57; e) X. Yang, D. He, X. He, K. Wang, J. Tang, Z. Zou, X. He, J. Xiong, L. Li, J. Shangguan, *ACS Appl. Mater. Interfaces* **2016**, *8*, 20558.

[53] S. Huh, J. W. Wiench, J.-C. Yoo, M. Pruski, V. S. Y. Lin, *Chem. Mater.* **2003**, *15*, 4247.

[54] T. Yu, A. Malugin, H. Ghandehari, *ACS Nano* **2011**, *5*, 5717.

[55] L. Li, T. Liu, C. Fu, L. Tan, X. Meng, H. Liu, *Nanomedicine* **2015**, *11*, 1915.

[56] J. Saikia, M. Yazdimamaghani, S. P. Hadipour Moghaddam, H. Ghandehari, *ACS Appl. Mater. Interfaces* **2016**, *8*, 34820.

[57] N. Hao, H. Liu, L. Li, D. Chen, L. Li, F. Tang, *J. Nanosci. Nanotechnol.* **2012**, *12*, 6346.

[58] R. C. Rowe, P. J. Sheskey, W. G. Cook, M. E. Fenton, *Handbook of Pharmaceutical Excipients*, Pharmaceutical Press, London **2012**.

[59] C. Wong, R. S. Bollampally, *J. Appl. Polym. Sci.* **1999**, *74*, 3396.

[60] a) Y. Hoshikawa, H. Yabe, A. Nomura, T. Yamaki, A. Shimojima, T. Okubo, *Chem. Mater.* **2010**, *22*, 12; b) A. M. Lipski, C. Jaquiery, H. Choi, D. Eberli, M. Stevens, I. Martin, I. W. Chen, V. P. Shastri, *Adv. Mater.* **2007**, *19*, 553; c) Y. Wei, D. Jin, D. J. Brennan, D. N. Rivera, Q. Zhuang, N. J. DiNardo, K. Qiu, *Chem. Mater.* **1998**, *10*, 769; d) J. Moghal, J. Kobler, J. Sauer, J. Best, M. Gardener, A. A. R. Watt, G. Wakefield, *ACS Appl. Mater. Interfaces* **2012**, *4*, 854.

[61] J.-Y. Choi, C. H. Park, J. Lee, *Drug Delivery* **2008**, *15*, 347.

[62] G. Costabile, I. d'Angelo, G. Rampioni, R. Bondì, B. Pompili, F. Ascenzioni, E. Mitidieri, R. d'Emmanuele di Villa Bianca, R. Sorrentino, A. Miro, F. Quaglia, F. Imperi, L. Leoni, F. Ungaro, *Mol. Pharmaceutics* **2015**, *12*, 2604.

[63] M. Kakran, R. Shegokar, N. G. Sahoo, L. Al Shaal, L. Li, R. H. Müller, *Eur. J. Pharm. Biopharm.* **2012**, *80*, 113.

[64] S. Barua, J.-W. Yoo, P. Kolhar, A. Wakankar, Y. R. Gokarn, S. Mitragotri, *Proc. Natl. Acad. Sci. USA* **2013**, *110*, 3270.

[65] C. Wischke, M. Schossig, A. Lendlein, *Small* **2014**, *10*, 83.

[66] D. M. Le, K. Kulangara, A. F. Adler, K. W. Leong, V. S. Ashby, *Adv. Mater.* **2011**, *23*, 3278.

[67] J. A. Champion, Y. K. Katare, S. Mitragotri, *Proc. Natl. Acad. Sci. USA* **2007**, *104*, 11901.

[68] R. A. Meyer, R. S. Meyer, J. J. Green, *J. Biomed. Mater. Res., Part A* **2015**, *103*, 2747.

[69] L. Chen, Z. Tian, Y. Du, *Biomaterials* **2004**, *25*, 3725.

[70] M. Caldorera-Moore, M. K. Kang, Z. Moore, V. Singh, S. V. Sreenivasan, L. Shi, R. Huang, K. Roy, *Soft Matter* **2011**, *7*, 2879.

[71] T. J. Merkel, K. Chen, S. W. Jones, A. A. Pandya, S. Tian, M. E. Napier, W. E. Zamboni, J. M. DeSimone, *J. Controlled Release* **2012**, *162*, 37.

[72] K. Chen, T. J. Merkel, A. Pandya, M. E. Napier, J. C. Luft, W. Daniel, S. Sheiko, J. M. DeSimone, *Biomacromolecules* **2012**, *13*, 2748.

[73] T. J. Merkel, S. W. Jones, K. P. Herlihy, F. R. Kersey, A. R. Shields, M. Napier, J. C. Luft, H. Wu, W. C. Zamboni, A. Z. Wang, J. E. Bear, J. M. DeSimone, *Proc. Natl. Acad. Sci. USA* **2011**, *108*, 586.

[74] F. R. Kersey, T. J. Merkel, J. L. Perry, M. E. Napier, J. M. DeSimone, *Langmuir* **2012**, *28*, 8773.

[75] K. Chen, J. Xu, J. C. Luft, S. Tian, J. S. Raval, J. M. DeSimone, *J. Am. Chem. Soc.* **2014**, *136*, 9947.

[76] J. L. Perry, K. G. Reuter, J. C. Luft, C. V. Pecot, W. Zamboni, J. M. DeSimone, *Nano Lett.* **2017**, *17*, 2879.

[77] K. J. Geh, M. Hubert, G. Winter, *J. Microencapsulation* **2016**, *33*, 595.

[78] S. A. Khan, M. Schneider, *Macromol. Biosci.* **2014**, *14*, 1627.

[79] P. Jurney, R. Agarwal, V. Singh, D. Choi, K. Roy, S. V. Sreenivasan, L. Shi, *J. Controlled Release* **2017**, *245*, 170.

[80] J. Zidek, J. Jancar, A. Milchev, T. A. Vilgis, *Macromolecules* **2014**, *47*, 8795.

[81] a) Y. Dong, H. Ruan, H. Wang, Y. Zhao, D. Bi, *J. Appl. Polym. Sci.* **2004**, *93*, 1553; b) F. S. Kittur, K. V. Harish Prashanth, K. Udaya Sankar, R. N. Tharanathan, *Carbohydr. Polym.* **2002**, *49*, 185.

[82] J. A. Champion, S. Mitragotri, in *Advances in Regenerative Medicine: Role of Nanotechnology, and Engineering Principles* (Eds: V. P. Shastri, G. Altankov, A. Lendlein), Springer, Dordrecht, Netherlands **2010**, p. 301.

[83] K. M. Keville, E. I. Franses, J. M. Caruthers, *J. Colloid Interface Sci.* **1991**, *144*, 103.

[84] D. A. Canelas, K. P. Herlihy, J. M. DeSimone, *Wiley Interdiscip. Rev.: Nanomed. Nanobiotechnol.* **2009**, *1*, 391.

[85] D. K. Hwang, J. Oakey, M. Toner, J. A. Arthur, K. S. Anseth, S. Lee, A. Zeiger, K. J. Van Vliet, P. S. Doyle, *J. Am. Chem. Soc.* **2009**, *131*, 4499.

[86] A. C. Anselmo, M. Zhang, S. Kumar, D. R. Vogus, S. Menegatti, M. E. Helgeson, S. Mitragotri, *ACS Nano* **2015**, *9*, 3169.

[87] A. Kyritsis, P. Pissis, J. L. Gómez Ribelles, M. Monleón Pradas, *J. Non-Cryst. Solids* **1994**, *172-174*, 1041.

[88] S. Kalakkunnath, D. S. Kalika, H. Lin, B. D. Freeman, *J. Polym. Sci., Part B: Polym. Phys.* **2006**, *44*, 2058.

[89] M. Caldorera-Moore, *Doctoral Dissertation*, The University of Texas at Austin, USA **2010**.

[90] C. H. Kapadia, S. Tian, J. L. Perry, J. C. Luft, J. M. DeSimone, *Mol. Pharmaceutics* **2016**, *13*, 3381.

[91] E. Riande, J. Guzmán, *Macromolecules* **1996**, *29*, 1728.

[92] S. Schubert, J. J. T. Delaney, U. S. Schubert, *Soft Matter* **2011**, *7*, 1581.

[93] C.-M. J. Hu, L. Zhang, S. Aryal, C. Cheung, R. H. Fang, L. Zhang, *Proc. Natl. Acad. Sci. USA* **2011**, *108*, 10980.

[94] P. Legrand, S. Lesieur, A. Bochot, R. Gref, W. Raatjes, G. Barratt, C. Vauthier, *Int. J. Pharm.* **2007**, *344*, 33.

[95] a) C.-M. J. Hu, R. H. Fang, J. Copp, B. T. Luk, L. Zhang, *Nat. Nanotechnol.* **2013**, *8*, 336; b) C.-M. J. Hu, R. H. Fang, B. T. Luk, L. Zhang, *Nat. Nanotechnol.* **2013**, *8*, 933.

[96] L. M. Cox, J. P. Killgore, Z. Li, R. Long, A. W. Sanders, J. Xiao, Y. Ding, *Langmuir* **2016**, *32*, 3691.

[97] B. Xu, Y. Q. Fu, M. Ahmad, J. K. Luo, W. M. Huang, A. Kraft, R. Reuben, Y. T. Pei, Z. G. Chen, J. T. M. De Hosson, *J. Mater. Chem.* **2010**, *20*, 3442.

[98] C. Palazzo, G. Ponchel, J. J. Vachon, S. Villebrun, F. Agnely, C. Vauthier, *Int. J. Polym. Mater. Polym. Biomater.* **2017**, *66*, 416.

[99] R. Mathaes, *Dissertation of Ludwig-Maximilians-Universität München*, Germany **2015**.

[100] M. Nagy, A. Keller, *Polym. Commun.* **1989**, *30*, 130.

[101] a) E. Enlow, *Doctoral Dissertation*, The University of North Carolina at Chapel Hill, USA **2010**; b) T. J. Merkel, *Doctoral Dissertation*, The University of North Carolina at Chapel Hill, USA **2011**; c) A. L. Galloway, A. Murphy, J. M. DeSimone, J. Di, J. P. Herrmann, M. E. Hunter, J. P. Kindig, F. J. Malinoski, M. A. Rumley, D. M. Stoltz, T. S. Templeman, B. Hubby, *Nanomedicine* **2013**, *9*, 523; d) K. Chen, *Doctoral Dissertation*, The University of North Carolina at Chapel Hill, USA **2013**.

[102] A. Besheer, J. Vogel, D. Glanz, J. Kressler, T. Groth, K. Mäder, *Mol. Pharmaceutics* **2009**, *6*, 407.

[103] H. M. Redhead, S. S. Davis, L. Illum, *J. Controlled Release* **2001**, *70*, 353.

[104] J. C. Neal, S. Stolnik, E. Schacht, E. R. Kenawy, M. C. Garnett, S. S. Davis, L. Illum, *J. Pharm. Sci.* **1998**, *87*, 1242.

[105] P. D. Scholes, A. G. A. Coombes, L. Illum, S. S. Davis, J. F. Watts, C. Ustariz, M. Vert, M. C. Davies, *J. Controlled Release* **1999**, *59*, 261.

[106] S. Staufenbiel, C. M. Keck, R. H. Müller, *Macromol. Symp.* **2014**, *345*, 32.

[107] L. Mu, S. S. Feng, *J. Controlled Release* **2002**, *80*, 129.

[108] K. Rechendorff, M. B. Hovgaard, M. Foss, V. P. Zhdanov, F. Besenbacher, *Langmuir* **2006**, *22*, 10885.

[109] a) T. Cedervall, I. Lynch, S. Lindman, T. Berggård, E. Thulin, H. Nilsson, K. A. Dawson, S. Linse, *Proc. Natl. Acad. Sci. USA* **2007**, *104*, 2050; b) F. Bertoli, D. Garry, M. P. Monopoli, A. Salvati, K. A. Dawson, *ACS Nano* **2016**, *10*, 10471.

[110] M. Hadjidemetriou, Z. Al-Ahmady, M. Mazza, R. F. Collins, K. Dawson, K. Kostarelos, *ACS Nano* **2015**, *9*, 8142.

[111] M. Hadjidemetriou, Z. Al-Ahmady, K. Kostarelos, *Nanoscale* **2016**, *8*, 6948.

[112] Y. Rharbi, *Phys. Rev. E* **2008**, *77*, 031806.

[113] D. Christie, C. Zhang, J. Fu, B. Koel, R. D. Priestley, *J. Polym. Sci., Part B: Polym. Phys.* **2016**, *54*, 1776.

[114] B. Bittner, M. Morlock, H. Koll, G. Winter, T. Kissel, *Eur. J. Pharm. Biopharm.* **1998**, *45*, 295.

[115] T. Unruh, H. Bunjes, K. Westesen, M. H. J. Koch, *J. Phys. Chem. B* **1999**, *103*, 10373.

[116] K. Westesen, H. Bunjes, *Int. J. Pharm.* **1995**, *115*, 129.

[117] a) G. Schmid, B. Corain, *Eur. J. Inorg. Chem.* **2003**, *2003*, 3081; b) P. Buffat, J. P. Borel, *Phys. Rev. A* **1976**, *13*, 2287.

[118] R. García-Álvarez, M. Hadjidemetriou, A. Sánchez-Iglesias, L. M. Liz-Marzán, K. Kostarelos, *Nanoscale* **2018**, *10*, 1256.

[119] M. Takagi, *J. Phys. Soc. Jpn.* **1954**, *9*, 359.

[120] Y. Yamamoto, K. Yasugi, A. Harada, Y. Nagasaki, K. Kataoka, *J. Controlled Release* **2002**, *82*, 359.

[121] Clariant; GmbH, (Ed: Clariant), Mowiol: Polyvinyl Alcohol, Commserv, Sulzbach, Germany **1999**.

[122] R. Ricciardi, F. Auriemma, C. De Rosa, F. Lauprêtre, *Macromolecules* **2004**, *37*, 1921.

[123] Y. Bin, Y. Tanabe, C. Nakabayashi, H. Kurosu, M. Matsuo, *Polymer* **2001**, *42*, 1183.

[124] C. Bouissou, J. J. Rouse, R. Price, C. F. van der Walle, *Pharm. Res.* **2006**, *23*, 1295.

[125] M. Thielen, K. Hartwig, P. Gust, *Blasformen von Kunststoffhohlkörpern*, Hanser, Munich, Germany **2006**.

[126] W. Weißbach, M. Dahms, *Werkstoffkunde: Strukturen, Eigenschaften, Prüfung*, Vieweg+Teubner Verlag, Wiesbaden, Germany **2007**.

[127] D. Quintanar-Guerrero, A. Ganem-Quintanar, E. Allémann, H. Fessi, E. Doelker, *J. Microencapsulation* **1998**, *15*, 107.

[128] M. A. Repka, J. W. McGinity, *Int. J. Pharm.* **2000**, *202*, 63.

[129] R. Gref, A. Domb, P. Quellec, T. Blunk, R. H. Müller, J. M. Verbavatz, R. Langer, *Adv. Drug Delivery Rev.* **1995**, *16*, 215.

[130] I. M. F. Campos, T. M. Santos, G. M. F. Cunha, K. M. M. N. Silva, R. Z. Domingues, A. da Silva Cunha Júnior, K. C. de Souza Figueiredo, *J. Appl. Polym. Sci.* **2014**, *131*, 41199.

[131] a) F. Siepmann, V. Le Brun, J. Siepmann, *J. Controlled Release* **2006**, *115*, 298; b) E. Piñón-Segundo, A. Ganem-Quintanar, V. Alonso-Pérez, D. Quintanar-Guerrero, *Int. J. Pharm.* **2005**, *294*, 217.

[132] L. Mu, S.-S. Feng, *Pharm. Res.* **2003**, *20*, 1864.

[133] L. Mu, S. S. Feng, *J. Controlled Release* **2003**, *86*, 33.

[134] M. F. Zambaux, F. Bonneaux, R. Gref, P. Maincent, E. Dellacherie, M. J. Alonso, P. Labrude, C. Vigneron, *J. Controlled Release* **1998**, *50*, 31.

[135] S. C. Lee, J. T. Oh, M. H. Jang, S. I. Chung, *J. Controlled Release* **1999**, *59*, 123.

[136] I. M. Adjei, B. Sharma, C. Peetla, V. Labhasetwar, *J. Controlled Release* **2016**, *232*, 83.

[137] W. Abdelwahed, G. Degobert, H. Fessi, *Int. J. Pharm.* **2006**, *309*, 178.

[138] Y. Lu, Y. Yin, Y. Xia, *Adv. Mater.* **2001**, *13*, 271.

[139] A. Banerjee, J. Qi, R. Gogoi, J. Wong, S. Mitragotri, *J. Controlled Release* **2016**, *238*, 176.

[140] O. Cauchois, *Doctoral Dissertation*, Université Paris Sud - Paris XI, France **2011**.

[141] H.-A. Klok, J. F. Langenwalter, S. Lecommandoux, *Macromolecules* **2000**, *33*, 7819.

[142] O. Cauchois, F. Segura-Sanchez, G. Ponchel, *Int. J. Pharm.* **2013**, *452*, 292.

[143] T. Jaworek, D. Neher, G. Wegner, R. H. Wieringa, A. J. Schouten, *Science* **1998**, *279*, 57.

[144] P. Papadopoulos, G. Floudas, I. Schnell, T. Aliferis, H. Iatrou, N. Hadjichristidis, *Biomacromolecules* **2005**, *6*, 2352.

[145] J. Tamayo, R. García, *Langmuir* **1996**, *12*, 4430.

[146] C. Q. Sun, *Prog. Solid State Chem.* **2007**, *35*, 1.

[147] Z. Yang, W. T. S. Huck, S. M. Clarke, A. R. Tajbakhsh, E. M. Terentjev, *Nat. Mater.* **2005**, *4*, 486.

[148] W. L. Lee, H. Y. Low, *Sci. Rep.* **2016**, *6*, 23686.

[149] Y. Wu, K. Wang, H. Tan, J. Xu, J. Zhu, *Langmuir* **2017**.

[150] R. Deng, F. Liang, W. Li, Z. Yang, J. Zhu, *Macromolecules* **2013**, *46*, 7012.

[151] I. Amin, M. Steenackers, N. Zhang, A. Beyer, X. Zhang, T. Pirzer, T. Hugel, R. Jordan, A. Gölzhäuser, *Small* **2010**, *6*, 1623.

[152] T. Dequivre, E. Al Alam, J. Plathier, A. Ruediger, G. Brisard, S. Charlebois, *ECS Trans.* **2015**, *69*, 91.

[153] H. Petrova, J. Perez-Juste, Z. Zhang, J. Zhang, T. Kosel, G. V. Hartland, *J. Mater. Chem.* **2006**, *16*, 3957.

[154] P. F. Kelly, *Properties of Materials*, CRC Press, Boca Raton, FL **2014**.

[155] R. Hoogenboom, *Macromol. Chem. Phys.* **2007**, *208*, 18.

[156] A. C. Moffat, M. D. Osselton, B. Widdop, *Clarke's Analysis of Drugs and Poisons: in Pharmaceuticals, Body Fluids and Postmortem Material*, Pharmaceutical Press, London **2011**.

[157] S. Lück, R. Schubel, J. Rüb, D. Hahn, E. Mathieu, H. Zimmermann, D. Scharnweber, C. Werner, S. Pautot, R. Jordan, *Biomaterials* **2016**, *79*, 1.

[158] A. Schulz, S. Jaksch, R. Schubel, E. Wegener, Z. Di, Y. Han, A. Meister, J. Kressler, A. V. Kabanov, R. Luxenhofer, C. M. Papadakis, R. Jordan, *ACS Nano* **2014**, *8*, 2686.

[159] Y. Han, Z. He, A. Schulz, T. K. Bronich, R. Jordan, R. Luxenhofer, A. V. Kabanov, *Mol. Pharmaceutics* **2012**, *9*, 2302.

[160] H. Bunjes, F. Steiniger, W. Richter, *Langmuir* **2007**, *23*, 4005.

[161] a) S. Hatziantoniou, G. Deli, Y. Nikas, C. Demetzos, G. T. Papaioannou, *Micron* **2007**, *38*, 819; b) H. Bunjes, M. H. J. Koch, K. Westesen, *J. Pharm. Sci.* **2003**, *92*, 1509.

[162] K. Göke, E. Roese, A. Arnold, J. Kuntsche, H. Bunjes, *Mol. Pharmaceutics* **2016**, *13*, 3187.

[163] C. Freitas, R. H. Müller, *Int. J. Pharm.* **1998**, *168*, 221.

[164] H. Bunjes, K. Westesen, M. H. J. Koch, *Int. J. Pharm.* **1996**, *129*, 159.

[165] F. Maleky, A. Marangoni, *Cryst. Growth Des.* **2011**, *11*, 2429.

[166] A. Radomska-Soukharev, *Adv. Drug Delivery Rev.* **2007**, *59*, 411.

[167] V. Krstic, U. Erb, G. Palumbo, *Scr. Metall. Mater.* **1993**, *29*, 1501.

[168] Q. Xu, A. Crossley, J. Czernuszka, *J. Pharm. Sci.* **2009**, *98*, 2377.

[169] a) R. Ni, U. Muenster, J. Zhao, L. Zhang, E.-M. Becker-Pelster, M. Rosenbruch, S. Mao, *J. Controlled Release* **2017**, *249*, 11; b) E. Allémann, J.-C. Leroux, R. Gurny, E. Doelker, *Pharm. Res.* **1993**, *10*, 1732.

[170] J. Shen, K. Lee, S. Choi, Y. Qu, Y. Wang, D. J. Burgess, *Int. J. Pharm.* **2016**, *498*, 274.

[171] Z. Ma, J. Bai, Y. Wang, X. Jiang, *ACS Appl. Mater. Interfaces* **2014**, *6*, 2431.

[172] C. E. Hall, O. Hall, *Lab. Invest.* **1963**, *12*, 721.

[173] a) T. Yamaoka, Y. Tabata, Y. Ikada, *J. Pharm. Pharmacol.* **1995**, *47*, 479; b) Y. Jiang, A. Schädlich, E. Amado, C. Weis, E. Odermatt, K. Mäder, J. Kressler, *J. Biomed. Mater. Res., Part B* **2010**, *93B*, 275.

[174] U.S. Food & Drug Administration, *Inactive Ingredient Search for Approved Drug Products*, FDA/Center for Drug Evaluation and Research, Silver Spring, MD, USA **2017**, https://www.accessdata.fda.gov/scripts/cder/iig/index.cfm (accessed: July 2019).

[175] E. Allémann, R. Gurny, E. Doelker, *Int. J. Pharm.* **1992**, *87*, 247.

[176] H. Ibrahim, C. Bindschaedler, E. Doelker, P. Buri, R. Gurny, *Int. J. Pharm.* **1992**, *87*, 239.

[177] Y. Dong, S.-S. Feng, *Int. J. Pharm.* **2007**, *342*, 208.

[178] M. N. V. Ravi Kumar, U. Bakowsky, C. M. Lehr, *Biomaterials* **2004**, *25*, 1771.

[179] R. V. Diaz, I. Soriano, A. Delgado, M. Llabrés, C. Evora, *J. Controlled Release* **1997**, *43*, 59.

[180] a) F. Yan, C. Zhang, Y. Zheng, L. Mei, L. Tang, C. Song, H. Sun, L. Huang, *Nanomedicine* **2010**, *6*, 170; b) Y. Dong, S.-S. Feng, *Biomaterials* **2005**, *26*, 6068; c) R. Gurny, N. A. Peppas, D. D. Harrington, G. S. Banker, *Drug Dev. Ind. Pharm.* **1981**, *7*, 1.

[181] P. Bihari, M. Vippola, S. Schultes, M. Praetner, A. G. Khandoga, C. A. Reichel, C. Coester, T. Tuomi, M. Rehberg, F. Krombach, *Part. Fibre Toxicol.* **2008**, *5*, 14.

[182] a) E. Allémann, J.-C. Leroux, R. Gurny, E. Doelker, *Eur. J. Pharm. Biopharm.* **1993**, *39*, 13; b) Y. N. Konan, R. Gurny, E. Allémann, *Int. J. Pharm.* **2002**, *233*, 239.

[183] H. J. van den Hul, J. W. Vanderhoff, *Br. Polym. J.* **1970**, *2*, 121.

[184] R. H. Müller, D. Rühl, M. Lück, B.-R. Paulke, *Pharm. Res.* **1997**, *14*, 18.

[185] D. Q. M. Craig, *Thermochim. Acta* **1995**, *248*, 189.

[186] Z. Chen, Z. Liu, F. Qian, *Mol. Pharmaceutics* **2015**, *12*, 590.

[187] J. Rühe, in *Polymer Brushes*, Wiley-VCH Verlag GmbH & Co. KGaA, Weinheim, Germany **2005**, p. 1.

[188] S. M. Moghimi, J. Szebeni, *Prog. Lipid Res.* **2003**, *42*, 463.

[189] I. Hamad, O. Al-Hanbali, A. C. Hunter, K. J. Rutt, T. L. Andresen, S. M. Moghimi, *ACS Nano* **2010**, *4*, 6629.

[190] M. Malmsten, B. Lassen, J. Westin, C.-G. Gölander, R. Larsson, U. R. Nilsson, *J. Colloid Interface Sci.* **1996**, *179*, 163.

[191] D. E. Owens III, N. A. Peppas, *Int. J. Pharm.* **2006**, *307*, 93.

[192] K. Sempf, T. Arrey, S. Gelperina, T. Schorge, B. Meyer, M. Karas, J. Kreuter, *Eur. J. Pharm. Biopharm.* **2013**, *85*, 53.

[193] M. S. Singh, A. Lamprecht, *Drug Dev. Ind. Pharm.* **2016**, *42*, 325.

[194] D. Quintanar-Guerrero, H. Fessi, E. Allémann, E. Doelker, *Int. J. Pharm.* **1996**, *143*, 133.

[195] E. Tyrode, M. W. Rutland, C. D. Bain, *J. Am. Chem. Soc.* **2008**, *130*, 17434.

[196] T. Sun, Y. S. Zhang, B. Pang, D. C. Hyun, M. Yang, Y. Xia, *Angew. Chem., Int. Ed.* **2014**, *53*, 12320.

[197] A. M. Alkilany, C. J. Murphy, *J. Nanopart. Res.* **2010**, *12*, 2313.

[198] M. Tebbe, C. Kuttner, M. Männel, A. Fery, M. Chanana, *ACS Appl. Mater. Interfaces* **2015**, *7*, 5984.

[199] C. Rulison, *KRUSS Application Report AR260e* **2007**, 1, https://www.kruss-scientific.com/fileadmin/user_upload/website/literature/kruss-ar260-en.pdf (accessed: July 2019).

[200] P. Ertl, B. Rohde, P. Selzer, *J. Med. Chem.* **2000**, *43*, 3714.

[201] I. Tuñón, E. Silla, J. L. Pascual-Ahuir, *Protein Eng., Des. Sel.* **1992**, *5*, 715.

[202] S. E. Feller, R. M. Venable, R. W. Pastor, *Langmuir* **1997**, *13*, 6555.

[203] K. Palm, P. Stenberg, K. Luthman, P. Artursson, *Pharm. Res.* **1997**, *14*, 568.

[204] S. V. F. Hansen, E. Christiansen, C. Urban, B. D. Hudson, C. J. Stocker, M. E. Due-Hansen, E. T. Wargent, B. Shimpukade, R. Almeida, C. S. Ejsing, M. A. Cawthorne, M. U. Kassack, G. Milligan, T. Ulven, *J. Med. Chem.* **2016**, *59*, 2841.

[205] B. Lee, F. M. Richards, *J. Mol. Biol.* **1971**, *55*, 379.

[206] J. Kelder, P. D. J. Grootenhuis, D. M. Bayada, L. P. C. Delbressine, J.-P. Ploemen, *Pharm. Res.* **1999**, *16*, 1514.

[207] D. E. Clark, *J. Pharm. Sci.* **1999**, *88*, 815.

[208] W. C. Griffin, *J. Soc. Cosmet. Chem.* **1949**, *1*, 311.

[209] L. Mu, P.-H. Seow, S.-N. Ang, S.-S. Feng, *Colloid Polym. Sci.* **2004**, *283*, 58.

[210] P.-Å. Albertsson, in *Advances in Protein Chemistry*, Vol. *24* (Eds: C. B. Anfinsen, J. T. Edsall, F. M. Richards), Academic Press, San Diego, CA **1970**, p. 309.

[211] R. H. Muller, S. S. Davis, L. Illum, E. Mak, in *Targeting of Drugs With Synthetic Systems* (Eds: G. Gregoriadis, J. Senior, G. Poste), Springer US, Boston, MA **1986**, p. 239.

[212] a) S. Stolnik, C. R. Heald, J. Neal, M. C. Garnett, S. S. Davis, L. Illum, S. C. Purkis, R. J. Barlow, P. R. Gellert, *J. Drug Targeting* **2001**, *9*, 361; b) S. Stolnik, S. E. Dunn, M. C. Garnett, M. C. Davies, A. G. A. Coombes, D. C. Taylor, M. P. Irving, S. C. Purkiss, T. F. Tadros, S. S. Davis, L. Illum, *Pharm. Res.* **1994**, *11*, 1800.

[213] J. Cheng, B. A. Teply, I. Sherifi, J. Sung, G. Luther, F. X. Gu, E. Levy-Nissenbaum, A. F. Radovic-Moreno, R. Langer, O. C. Farokhzad, *Biomaterials* **2007**, *28*, 869.

[214] a) Y.-P. Li, Y.-Y. Pei, X.-Y. Zhang, Z.-H. Gu, Z.-H. Zhou, W.-F. Yuan, J.-J. Zhou, J.-H. Zhu, X.-J. Gao, *J. Controlled Release* **2001**, *71*, 203; b) Y. Choi, S. Yoon Kim, M.-H. Moon, S. Hee Kim, K.-S. Lee, Y. Byun, *Biomaterials* **2001**, *22*, 995.

[215] a) C. Li, E. Coons, A. Strachan, *Acta Mech.* **2014**, *225*, 1187; b) J. Bicerano, *Prediction of Polymer Properties*, CRC Press, Boca Raton, FL **2002**.

[216] A. A. Metwally, R. M. Hathout, *Mol. Pharmaceutics* **2015**, *12*, 2800.

[217] M. S. Dresselhaus, G. Dresselhaus, P. C. Eklund, *Science of Fullerenes and Carbon Nanotubes: Their Properties and Applications*, Elsevier Science, Amsterdam **1996**.

[218] M. Treacy, T. Ebbesen, J. Gibson, *Nature* **1996**, *381*, 678.

[219] S. Iijima, *Nature* **1991**, *354*, 56.

[220] Y. Xiao, M. R. Wiesner, *J. Hazard. Mater.* **2012**, *215-216*, 146.

[221] J. A. Brant, J. Labille, J.-Y. Bottero, M. R. Wiesner, *Langmuir* **2006**, *22*, 3878.

[222] M. F. Islam, E. Rojas, D. M. Bergey, A. T. Johnson, A. G. Yodh, *Nano Lett.* **2003**, *3*, 269.

[223] D. K. Owens, R. C. Wendt, *J. Appl. Polym. Sci.* **1969**, *13*, 1741.

[224] a) B. Jańczuk, J. M. Bruque, M. L. González-Martin, E. Román-Galán, *Colloids Surf., A* **1995**, *100*, 93; b) D. K. Owens, *J. Appl. Polym. Sci.* **1970**, *14*, 1725.

[225] B. Jańczuk, M. L. González-Martín, J. M. Bruque, C. Dorado-Calasanz, J. M. del Pozo, *J. Colloid Interface Sci.* **1995**, *176*, 352.

[226] B. Jańczuk, M. L. Kerkeb, T. Biatrowicz, F. González-Caballero, *J. Colloid Interface Sci.* **1992**, *151*, 333.

[227] a) O. Planinšek, R. Pišek, A. Trojak, S. Srčič, *Int. J. Pharm.* **2000**, *207*, 77; b) G. E. Parsons, G. Buckton, S. M. Chatham, *Int. J. Pharm.* **1992**, *82*, 145; c) W. Abdelwahed, G. Degobert, H. Fessi, *Eur. J. Pharm. Biopharm.* **2006**, *63*, 87; d) W. Abdelwahed, G. Degobert, H. Fessi, *Int. J. Pharm.* **2006**, *324*, 74.

[228] C. J. van Oss, R. J. Good, *J. Macromol. Sci., Part A: Chem.* **1989**, *26*, 1183.

[229] R. J. Chokshi, H. Zia, H. K. Sandhu, N. H. Shah, W. A. Malick, *Drug Delivery* **2007**, *14*, 33.

[230] a) C. Weber, C. Coester, J. Kreuter, K. Langer, *Int. J. Pharm.* **2000**, *194*, 91; b) K. Langer, S. Balthasar, V. Vogel, N. Dinauer, H. von Briesen, D. Schubert, *Int. J. Pharm.* **2003**, *257*, 169; c) C. J. Van Oss, R. J. Good, M. K. Chaudhury, *J. Chromatogr. A* **1987**, *391*, 53.

[231] a) E. Fattal, C. Vauthier, I. Aynie, Y. Nakada, G. Lambert, C. Malvy, P. Couvreur, *J. Controlled Release* **1998**, *53*, 137; b) F. Varenne, A. Makky, M. Gaucher-Delmas, F. Violleau, C. Vauthier, *Pharm. Res.* **2016**, *33*, 1220.

[232] J. Bergendahl, D. Grasso, *AIChE J.* **1999**, *45*, 475.

[233] a) F. J. Holly, M. F. Refojo, in *Hydrogels for Medical and Related Applications*, Vol. *31*, American Chemical Society, Washington, DC, USA **1976**, p. 252; b) M. Pérez Olmedilla, N. Garcia-Giralt, M. M. Pradas, P. B. Ruiz, J. L. Gómez Ribelles, E. C. Palou, J. C. M. García, *Biomaterials* **2006**, *27*, 1003.

[234] a) J. Guan, C. Gao, L. Feng, J. Sheng, *J. Biomater. Sci., Polym. Ed.* **2000**, *11*, 523; b) D. E. Rice, J. V. Ihlenfeld, *Google Patents (US4440918)*, **1984**.

[235] M. Ebara, J. M. Hoffman, P. S. Stayton, A. S. Hoffman, *Radiat. Phys. Chem.* **2007**, *76*, 1409.

[236] G. Tan, R. Chen, C. Ning, L. Zhang, X. Ruan, J. Liao, *J. Appl. Polym. Sci.* **2012**, *124*, 459.

[237] I.-K. Kang, Y. Ito, M. Sisido, Y. Imanishi, *Polym. J.* **1987**, *19*, 1329.

[238] S. K. H. Reinke, K. Hauf, J. Vieira, S. Heinrich, S. Palzer, *J. Phys. D: Appl. Phys.* **2015**, *48*, 464001.

[239] A. Voronov, A. Kohut, W. Peukert, S. Voronov, O. Gevus, V. Tokarev, *Langmuir* **2006**, *22*, 1946.

[240] P. Kim, K. Y. Suh, *Langmuir* **2007**, *23*, 4549.

[241] a) S. Wang, Y. Zhang, N. Abidi, L. Cabrales, *Langmuir* **2009**, *25*, 11078; b) X. Wang, Q. Li, J. Xie, Z. Jin, J. Wang, Y. Li, K. Jiang, S. Fan, *Nano Lett.* **2009**, *9*, 3137; c) J. T. Cang-Rong, G. Pastorin, *Nanotechnology* **2009**, *20*, 255102.

[242] a) G. Tripodo, C. Wischke, A. Lendlein, *Macromol. Symp.* **2011**, *309-310*, 49; b) A. B. W. Brochu, G. A. Evans, W. M. Reichert, *J. Biomed. Mater. Res., Part B* **2014**, *102*, 181.

[243] C. A. Kienzle-Sterzer, D. Rodriguez-Sanchez, C. Rha, *Makromol. Chem.* **1982**, *183*, 1353.

[244] D. Armani, C. Liu, N. Aluru, presented at Technical Digest. IEEE Int. MEMS 99 Conf. 12th IEEE Int. Conf. on Micro Electro Mechanical Systems (Cat. No.99CH36291), Orlando, FL, USA, January **1999**.

[245] Y.-C. Tseng, S.-H. Hyon, Y. Ikada, *Biomaterials* **1990**, *11*, 73.

[246] S. Janssens, S. Nagels, H. N. d. Armas, W. D'Autry, A. Van Schepdael, G. Van den Mooter, *Eur. J. Pharm. Biopharm.* **2008**, *69*, 158.

[247] L. Mu, M.-M. Teo, H.-Z. Ning, C.-S. Tan, S.-S. Feng, *J. Controlled Release* **2005**, *103*, 565.

[248] P. K. Jana, S. P. Moulik, *J. Phys. Chem.* **1991**, *95*, 9525.

[249] W. G. Chambliss, R. W. Cleary, R. Fischer, A. B. Jones, P. Skierkowski, W. Nicholes, A. H. Kibbe, *J. Pharm. Sci.* **1981**, *70*, 1248.

[250] A. Chattopadhyay, E. London, *Anal. Biochem.* **1984**, *139*, 408.

[251] M. Ash, I. Ash, *Handbook of Industrial Surfactants*, Synapse Information Resources, Endicott, NY, USA **2010**.

[252] United States Environmental Protection Agency (EPA), Chemistry Dashboard, https://comptox.epa.gov/dashboard/, **2017**, (accessed: July 2019).

[253] A. Roda, A. F. Hofmann, K. J. Mysels, *J. Biol. Chem.* **1983**, *258*, 6362.

[254] A. M. Al-mahallawi, O. M. Khowessah, R. A. Shoukri, *Int. J. Pharm.* **2014**, *472*, 304.

[255] a) A. Patist, S. S. Bhagwat, K. W. Penfield, P. Aikens, D. O. Shah, *J. Surfactants Deterg.* **2000**, *3*, 53; b) B. A. Kerwin, *J. Pharm. Sci.* **2008**, *97*, 2924.

[256] L. S. C. Wan, P. F. S. Lee, *J. Pharm. Sci.* **1974**, *63*, 136.

[257] M. J. Schwuger, *J. Colloid Interface Sci.* **1973**, *43*, 491.

[258] B. Geetha, A. B. Mandal, T. Ramasami, *Macromolecules* **1993**, *26*, 4083.

[259] I. Matsaridou, P. Barmpalexis, A. Salis, I. Nikolakakis, *AAPS PharmSciTech* **2012**, *13*, 1319.

[260] MarvinSketch, (Version 17.1.23.0), ChemAxon, http://www.chemaxon.com, Budapest **2017**.

[261] T. B. Rosenthal, *J. Biol. Chem.* **1948**, *173*, 25.

[262] a) P. Allsop, M. Cheetham, S. Brooks, G. M. Hall, C. Williams, *Eur. J. Appl. Physiol. Occup. Physiol.* **1990**, *59*, 465; b) M. G. Dickson, D. T. Sharpe, *Br. J. Plast. Surg.* **1985**, *38*, 39.

[263] D. Street, J. Bangsbo, C. Juel, *J. Physiol.* **2001**, *537*, 993.

[264] H. Rachmawati, B. M. Haryadi, K. Anggadiredja, V. Suendo, *AAPS PharmSciTech* **2015**, *16*, 692.

[265] H. Ando, A. Okamoto, M. Yokota, T. Asai, T. Dewa, N. Oku, *J. Gene Med.* **2013**, *15*, 375.

[266] K. Hu, J. Li, Y. Shen, W. Lu, X. Gao, Q. Zhang, X. Jiang, *J. Controlled Release* **2009**, *134*, 55.

[267] S. Barua, S. Mitragotri, *ACS Nano* **2013**, *7*, 9558.

[268] S. Tenzer, D. Docter, J. Kuharev, A. Musyanovych, V. Fetz, R. Hecht, F. Schlenk, D. Fischer, K. Kiouptsi, C. Reinhardt, K. Landfester, H. Schild, M. Maskos, S. K. Knauer, R. H. Stauber, *Nat. Nanotechnol.* **2013**, *8*, 772.

[269] B. M. Haryadi, G. Winter, J. Engert, *Unpublished* **2019**.

[270] B. A. Webb, M. Chimenti, M. P. Jacobson, D. L. Barber, *Nat. Rev. Cancer* **2011**, *11*, 671.

[271] J. Buske, C. König, S. Bassarab, A. Lamprecht, S. Mühlau, K. G. Wagner, *Eur. J. Pharm. Biopharm.* **2012**, *81*, 57.

[272] D. Bazile, C. Prud'homme, M.-T. Bassoullet, M. Marlard, G. Spenlehauer, M. Veillard, *J. Pharm. Sci.* **1995**, *84*, 493.

[273] T. G. Park, S. Cohen, R. Langer, *Macromolecules* **1992**, *25*, 116.

[274] a) T. Ishida, R. Maeda, M. Ichihara, K. Irimura, H. Kiwada, *J. Controlled Release* **2003**, *88*, 35; b) T. Ishida, K. Masuda, T. Ichikawa, M. Ichihara, K. Irimura, H. Kiwada, *Int. J. Pharm.* **2003**, *255*, 167.

[275] A. C. Anselmo, V. Gupta, B. J. Zern, D. Pan, M. Zakrewsky, V. Muzykantov, S. Mitragotri, *ACS Nano* **2013**, *7*, 11129.

[276] H. Yoshino, M. Kobayashi, M. Samejima, *Chem. Pharm. Bull.* **1983**, *31*, 237.

[277] a) J. W. Donovan, *Biopolymers* **1979**, *18*, 263; b) N. I. Khitarov, A. A. Kadik, *Contrib. Mineral. Petrol.* **1973**, *41*, 205.

[278] EDQM, European Pharmacopoeia, 9th Edition, Including Subscription to Supplement 9.6-9.8, Council of Europe, European

Pharmacopoeia Commission, European Directorate for the Quality of Medicines & Healthcare, Strasborug, France **2019**.

[279] USPC, USP 41 - NF 36 The United States Pharmacopeia and National Formulary: Main Edition Plus Supplements 1 and 2, United States Pharmacopeial Convention, North Bethesda, MD, USA **2018**.

[280] BPC, British Pharmacopoeia 2016 (BP 2016), British Pharmacopoeia Commission, London, UK **2015**.

[281] G. Dalwadi, H. A. E. Benson, Y. Chen, *Pharm. Res.* **2005**, *22*, 2152.

[282] Y. Shen, M. Y. Gee, A. B. Greytak, *Chem. Commun.* **2017**, *53*, 827.

[283] WHO, The International Pharmacopoeia, 8th Edition, World Health Organization, Geneva, Switzerland **2018**.

[284] Pharmaceutical and Medical Device Regulatory Science Foundation, *Japanese Pharmacopoeia*, 17th ed., The Ministry of Health, Labour and Welfare, Tokyo, Japan **2016**.

[285] EMA, Note for guidance on limitations to the use of ethylene oxide in the manufacture of medicinal products (CPMP/QWP/159/01) (EMEA/CVMP/271/01 Rev. 1), European Medicines Agency, London, UK **2016**, 1.

[286] H. E. Williams, J. Huxley, M. Claybourn, J. Booth, M. Hobbs, E. Meehan, B. Clark, *Polym. Degrad. Stab.* **2006**, *91*, 2171.

[287] H. Shearer, M. J. Ellis, S. P. Perera, J. B. Chaudhuri, *Tissue Eng.* **2006**, *12*, 2717.

[288] a) M. Goldman, R. Gronsky, G. G. Long, L. Pruitt, *Polym. Degrad. Stab.* **1998**, *62*, 97; b) B. Burton, A. Gaspar, D. Josey, J. Tupy, M. D. Grynpas, T. L. Willett, *Bone* **2014**, *61*, 71.

[289] a) M. Shameem, H. Lee, K. Burton, B. C. Thanoo, P. P. Deluca, *PDA J. Pharm. Sci. Technol.* **1999**, *53*, 309; b) L. Montanari, M. Costantini, E. C. Signoretti, L. Valvo, M. Santucci, M. Bartolomei, P. Fattibene, S. Onori, A. Faucitano, B. Conti, I. Genta, *J. Controlled Release* **1998**, *56*, 219; c) A. Lendlein, M. Behl, B. Hiebl, C. Wischke, *Expert Rev. Med. Devices* **2010**, *7*, 357.

[290] W. Friess, M. Schlapp, *Eur. J. Pharm. Biopharm.* **2006**, *63*, 176.

[291] A. Castoldi, M. Empting, C. De Rossi, K. Mayr, P. Dersch, R. Hartmann, R. Müller, S. Gordon, C.-M. Lehr, *Pharm. Res.* **2019**, *36*, 22.